NAVAL POSTGRADUATE SCHOOL
Monterey, California

THESIS

Thermodynamic and Dynamic Processes
in the Updraft Region
of GALE IOP9

by

Dianne K. Crittenden

March 1989

Thesis Advisor: Wendell A. Nuss

REPORT DOCUMENTATION PAGE

1a Report Security Classification: Unclassified		1b Restrictive Markings	
2a Security Classification Authority		3 Distribution/Availability of Report: Approved for public release; distribution is unlimited.	
2b Declassification Downgrading Schedule			
4 Performing Organization Report Number(s)		5 Monitoring Organization Report Number(s)	
6a Name of Performing Organization: Naval Postgraduate School	6b Office Symbol (if applicable): 35	7a Name of Monitoring Organization: Naval Postgraduate School	
6c Address (city, state, and ZIP code): Monterey, CA 93943-5000		7b Address (city, state, and ZIP code): Monterey, CA 93943-5000	
8a Name of Funding Sponsoring Organization	8b Office Symbol (if applicable)	9 Procurement Instrument Identification Number	
8c Address (city, state, and ZIP code)		10 Source of Funding Numbers: Program Element No / Project No / Task No / Work Unit Accession No	

11 Title (Include security classification): THERMODYNAMIC AND DYNAMIC PROCESSES IN THE UPDRAFT REGION OF GALE IOP9

12 Personal Author(s): Dianne K. Crittenden

13a Type of Report	13b Time Covered	14 Date of Report (year, month, day)	15 Page Count
Master's Thesis	From To	March 1989	55

16 Supplementary Notation: The views expressed in this thesis are those of the author and do not reflect the official policy or position of the Department of Defense or the U.S. Government.

17 Cosati Codes			18 Subject Terms (continue on reverse if necessary and identify by block number)
Field	Group	Subgroup	Meteorology, Explosive Cyclogenesis, GALE

19 Abstract (continue on reverse if necessary and identify by block number)

A detailed diagnostic examination of the warm frontal region ahead of the surface cyclone in Intensive Observation Period (IOP) 9 of the Genesis of Atlantic Lows Experiment (GALE) is conducted. Data for this study consists of normal synoptic observations and special GALE observations, analyzed by the Navy Operational Regional Analysis and Prediction System (NORAPS), which uses optimal interpolation. These analyses are enhanced by hand-drawn fronts and cloud outlines from Geostationary Operational Environmental Satellite (GOES) imagery. Symmetric stability is evaluated on cross-sectional analyses of pseudo-absolute momentum and equivalent potential temperature, and reveal conditions of moist symmetric neutrality in the warm frontal region. The planetary boundary layer θ_e budget is examined to determine what processes heated and moistened the region. Surface heat and moisture fluxes were found to contribute to significant θ_e increases only in the early stages of development. Upper-level divergence and surface frontogenesis are studied to determine their contributions to forcing the warm frontal updraft. Results indicate that during the period of explosive development, upper-level forcing was unfavorable for development. Low-level frontogenetical forcing in the presence of symmetric neutrality was found to be strong enough to oppose this negative upper-level forcing to force rapid development.

20 Distribution Availability of Abstract	21 Abstract Security Classification	
☒ unclassified unlimited ☐ same as report ☐ DTIC users	Unclassified	
22a Name of Responsible Individual: Wendell A. Nuss	22b Telephone (include Area code): (408) 646-2044	22c Office Symbol: 63Nu

DD FORM 1473,84 MAR — 83 APR edition may be used until exhausted; All other editions are obsolete

Approved for public release; distribution is unlimited.

Thermodynamic and Dynamic Processes in the Updraft
Region of GALE IOP9

by

Dianne K. Crittenden
Lieutenant, United States Navy
B.S., University of Missouri, 1982

Submitted in partial fulfillment of the
requirements for the degree of

MASTER OF SCIENCE IN METEOROLOGY AND OCEANOGRAPHY

from the

NAVAL POSTGRADUATE SCHOOL
March 1989

ABSTRACT

A detailed diagnostic examination of the warm frontal region ahead of the surface cyclone in Intensive Observation Period (IOP) 9 of the Genesis of Atlantic Lows Experiment (GALE) is conducted. Data for this study consists of normal synoptic observations and special GALE observations, analyzed by the Navy Operational Regional Analysis and Prediction System (NORAPS), which uses optimal interpolation. These analyses are enhanced by hand-drawn fronts and cloud outlines from Geostationary Operational Environmental Satellite (GOES) imagery. Symmetric stability is evaluated on cross-sectional analyses of pseudo-absolute momentum and equivalent potential temperature, and reveal conditions of moist symmetric neutrality in the warm frontal region. The planetary boundary layer θ_e budget is examined to determine what processes heated and moistened the region. Surface heat and moisture fluxes were found to contribute to significant θ_e increases only in the early stages of development. Upper-level divergence and surface frontogenesis are studied to determine their contributions to forcing the warm frontal updraft. Results indicate that during the period of explosive development, upper-level forcing was unfavorable for development. Low-level frontogenetical forcing in the presence of symmetric neutrality was found to be strong enough to oppose this negative upper-level forcing to force rapid development.

TABLE OF CONTENTS

LIST OF FIGURES

I. INTRODUCTION

A. BACKGROUND

Explosive cyclogenesis poses serious problems for the forecaster. Explosive development has been defined by Sanders and Gyakum (1980) as a 24-h drop in central pressure of 24-mb at 60 ° N and is adjusted for geostrophic equivalency at an arbitrary latitude, (ϕ), by multiplying by ($\frac{\sin \phi}{\sin 60}$). The distinction between these and non-explosive developing cyclones is made because of their severe weather. Primarily maritime events occurring in western oceans, explosive cyclones have caused injury, death and property damage in coastal areas and on naval and merchant vessels at sea.

Explosive cyclones are often poorly predicted by numerical forecast models due in part to a lack of understanding of their development. Past studies of explosive cyclogenesis have attempted to isolate the dynamic effects that lead to rapid development. Upper-level baroclinic processes undoubtedly play a dominant role in explosive development, as suggested by the climatological study of Sanders (1986a) and numerous case studies. The importance of surface and boundary layer processes has also been illustrated in a climatological study by Davis and Emanuel (1988) and other case studies. Various mechanisms can be shown to contribute to explosive cyclogenesis, but such a complex phenomenon is more likely the result of an interaction between the dominant baroclinic processes and diabatic effects associated with the surface heat and moisture fluxes.

Individual case studies have identified the mechanisms by which upper level forcing contributes to explosive cyclogenesis. In their analysis of an explosive cyclone over the eastern United States, Boyle and Bosart (1986) examined the synoptic-scale upper-level thermal and vorticity advection. They found that strong cold air advection above 500-mb into the trough accompanied rapid cyclogenesis at the surface. Subsidence associated with the cold advection was greatest at 500-mb, causing vortex tube stretching, which generated cyclonic vorticity above 500-mb. The strong cyclonic vorticity generated at these levels was advected downstream and enhanced development of the surface cyclone.

Uccellini et al. (1985) have shown that smaller-scale upper-level baroclinic processes associated with jet streaks enhanced the vertical circulation and cyclogenesis in the 1979 President's Day storm. The mechanism for this forcing is convincingly demonstrated in

numerical simulations of the same storm by Uccellini et al. (1987) and Whittaker et al. (1988). They found that strong divergence associated with the upper-level jet induced a secondary circulation that extended throughout the depth of the troposphere. The jet-induced circulation enhanced the development of a low-level jet and secondary cyclogenesis at the surface.

The process by which the planetary boundary layer (PBL) and surface heat and moisture fluxes influence explosive cyclongenesis is less certain. However, individual case studies reveal possible mechanisms for surface flux influences on explosive cyclogenesis. Of particular interest is the interaction between static stability, surface fluxes, surface fronts and baroclinic processes. Baroclinic theory indicates that disturbances grow more rapidly when the static stability of the atmosphere is small. Reed and Albright (1986) investigated an explosive cyclogenesis event in the eastern North Pacific Ocean in 1981. Their analyses of changes in surface temperature and dew-point temperature revealed that the surface temperature and moisture increased in the vicinity of surface cyclone development. The 500-mb temperature also increased, but by a smaller amount, resulting in a reduction of the static stability. The reduced static stability was believed to have been caused in part by advection of high equivalent potential temperature (θ_e) air ahead of the cyclone and by warming and moistening of the PBL by surface heat and moisture fluxes.

Bosart and Lin (1984) performed a diagnostic analysis of the 1979 President's Day storm in which sensible and latent heat fluxes were analyzed. They concluded that oceanic heat fluxes were vital to cyclogenesis prior to frontal development. Atlas (1987) examined the roles of the surface fluxes in numerical predictions of the same storm. A forecast without any surface fluxes failed to predict any surface development. Adding just heat fluxes to the model resulted in weak development. The model run with both heat and moisture fluxes accurately predicted the cyclogenesis. He concluded that the surface fluxes decreased the static stability, generated low-level cyclonic vorticity, and increased baroclinicity in the vicinity of cyclone development. Model simulations by Uccellini et al. (1987) confirm this interpretation of the role of the surface fluxes and also found that the fluxes contributed to latent heat release in the jet streak forced circulation.

While interaction between surface fluxes, diabatic heating and jet streaks is clear for the President's Day storm on a coastal front, the interaction of these processes has not been clearly shown for cyclones over the open ocean. In open ocean cyclones, the warm frontal region is likely to be the focal point of this interaction as suggested by Nuss

(1989). Emanuel (1988) indicated that this ascent region is characterized by moist slantwise neutrality. In a recent study of frontal circulations under conditions where the atmosphere was neutral to slantwise convection, Emanuel (1985) solved the Sawyer-Eliassen equation for the case where the potential vorticity, q, approached zero. The result of the frontogenetical forcing was to force a strong, small scale updraft on the warm side of the maximum temperature gradient. Sanders (1986b) found observational evidence of a strong narrow updraft in his analysis of a New England snowstorm in 1981. The atmosphere ahead of the storm center was characterized by small, nearly neutral symmetric stability and strong frontogenetical forcing. He concluded that frontogenesis drove a strong band of ascent above the surface and that small symmetric stability enhanced the intensity of the frontal circulation. These studies suggest that processes associated with the warm front may also contribute to enhanced cyclogenesis.

The intent of this thesis is to look at one particular case of oceanic explosive cyclogenesis in terms of the dynamic and thermodynamic forcing mechanisms and of the interactions between the mechanisms. Several questions will be studied: Was moist symmetric neutrality present in the vicinity of the surface warm front? How did the PBL structure influence surface frontogenesis? Did strong warm frontogenesis enhance the upper- level jet to aid surface cyclone development? What contributions did surface fluxes make to increasing the heat and moisture in the warm frontal updraft region?

B. GENESIS OF ATLANTIC LOWS EXPERIMENT (GALE)

From 15 January to 15 March 1986, the Genesis of Atlantic Lows Experiment (GALE) was conducted as an effort to study mesoscale processes in winter cyclones. GALE was a cooperative experiment undertaken by several agencies and universities to collect data with a higher spatial resolution than is available with the standard synoptic data network. According to the GALE Field Program Summary (1986), the GALE objectives were to study mesoscale processes and the influence of air-sea interactions in cyclogenesis over the east coast of the United States. The GALE data network was centered over the Carolinas. The field experiment was divided into 13 Intensive Observing Periods (IOP's), during which special observations were taken throughout the eastern United States, including an area extending several hundred miles offshore.

This thesis deals with GALE IOP9, which covered a 49-h period from 1800 UTC 24 February through 1900 UTC 26 February. During IOP9, an explosive cyclogenesis event occurred off the East Coast. Pertle (1987) has described synoptic and subsynoptic processes occurring during IOP9 and conducted a verification of the Navy Operational

Regional Analysis and Prediction System (NORAPS) forecasts of the system. Carson (1988) further refined the synoptic-scale development of this oceanic cyclone and indicated that low static stability was present in the region of this cyclone.

The goal of this thesis is to look at the detailed thermodynamic processes and forcing mechanisms that may have contributed to the rapid cyclogenesis in GALE IOP9. In particular, the interaction of surface- and upper-level forcing mechanisms in the warm frontal region will be examined. Specific goals include:

1. Demostrate the presence of small symmetric stability in IOP9 ahead of the surface cyclone in the vicinity of the warm front.
2. Determine the contribution by the surface fluxes to increasing the surface potential temperature (θ_e) in the updraft region
3. Examine the forcing mechanisms in the updraft region
4. Examine the relationship between upper-level forcing, surface frontogenesis and symmetric neutrality in producing strong ascent along the warm front.

C. DATA AND ANALYSIS

The analyses used for this study are prepared by NORAPS, using an optimal interpolation (OI) method to convert a field of meteorological observations into a set of data grid points. Values are weighted depending on the distance between observation and grid point, type of observation, age of observation and density of observations around the grid point. Data from the normal synoptic network were supplemented by special GALE data.

To highlight key dynamical features, subjectively enhanced analyses were made from the numerical analyses, individual observations and Geostationary Environmental Operational Satellite (GOES) imagery. Sea-level pressure charts were modified by hand to depict accurate cyclone center positions and intensities. In addition, fronts and cloud outlines were added to the gridded surface analyses. The surface features were enhanced for a detailed analysis of IOP9 performed by Wash, et al. (1989).

Because of the additional observations and the subjective modifications, the final analyses used in this study depict more detail than is usually the case for oceanic regions. However, there are limitations to the data which must be considered before drawing conclusions. First, the NORAPS analyses have an 80-km grid resolution, which is too coarse to resolve details of small-scale features. Second, the moisture fields used in the model analyses are 12-h forecast fields. Consequently, some of the conclusions drawn may include inherent uncertainties. Where possible, the uncertainties have been noted and evaluated and the analyses are considered sound.

II. SYNOPTIC DISCUSSION

Complete discussions of the synoptic-scale forcing and evolution of this cyclone are available in Pertle (1987) and Carson (1988). Key aspects of the synoptic evolution that relate to the circulation in the warm frontal region are highlighted in the following sections.

A. 1200 UTC 24 FEBRUARY 1986

Key upper-level features for this pre-cyclogenesis period were a 500-mb shortwave trough (not shown) that extended from Lake Michigan through Mississippi and a strong upper-level jet that extended from the Gulf Coast across southern Georgia and then offshore. An area of large positive vorticity associated with the trough existed with a maximum of $22 \times 10^{-5} s^{-1}$ centered over the Ohio River Valley, with the strongest positive vorticity advection (PVA) over Kentucky. The trough at 250-mb was located near the 500-mb trough location. Downstream from this 250-mb trough, near the Florida panhandle, a 70-m/s jet streak enhanced the positive vorticity in the trough (Fig. 1). Another jet streak, with a 60-m/s maximum, was located offshore, from 32 ° N 68 ° W to 37 ° N 60 ° W. The surface analysis showed a weak cyclone was centered over Kentucky (Fig. 2) under the PVA region of the 500-mb short wave trough. A 998-mb low off Nova Scotia produced a trailing cold front that extended through a secondary low near 38 ° N 56 ° W, southwestward to the tip of Florida. Frontal positions were taken from Wash, et al. (1989).

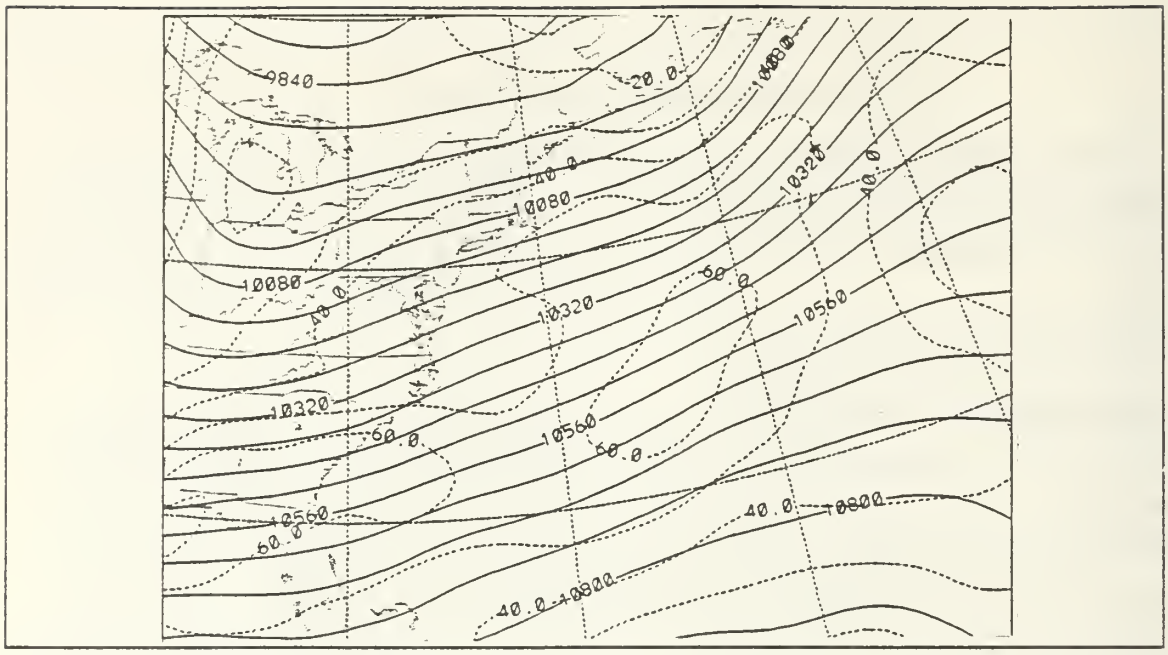

Figure 1. **1200 UTC 24 February 1986 Upper-Level Analysis:** NORAPS analysis of 250-mb heights, m (solid) and isotachs, m/s (dashed).

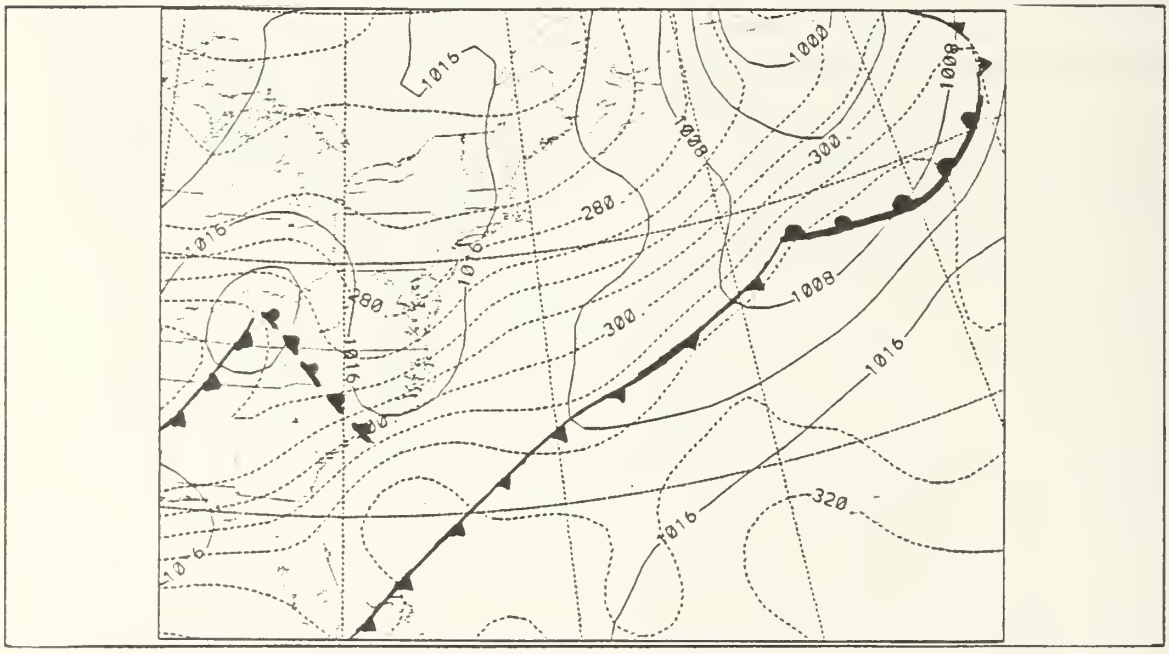

Figure 2. **1200 UTC 24 February 1986 Surface Analysis:** Sfc pressure, mb (solid) and θ_e, K (dashed).

B. 0000 UTC 25 FEBRUARY 1986

The jet and shortwave trough advanced eastward (Fig. 3) to produce an area of positive vorticity with a maximum of $22 \times 10^{-5} s^{-1}$ over the Carolinas, which provided strong PVA offshore. The jet maximum was greater than 70-m/s at 250-mb just off the east coast of Florida offshore to near 34 ° N 71 ° W. Downstream, a smaller jet streak with a maximum of 60-m/s was centered near 37 ° N 60 ° W. The surface low previously over Kentucky deepened to a central pressure of 1007-mb and apparently moved off the coast of North Carolina (Fig. 4). However, careful hand analysis by Carson (1988) revealed the development of a distinct second low further offshore, which subsequently developed rapidly. A cold front trailed through the Carolinas and Georgia then along the Gulf Coast. The clouds added to the analysis by Carson (1988) and Wash, et al. (1989) showed that this second low was clearly separate from a comma cloud associated with the left exit region of the jet streak. It will be shown in this study that this second low developed along a region of warm frontogenesis in an environment of small symmetric stability.

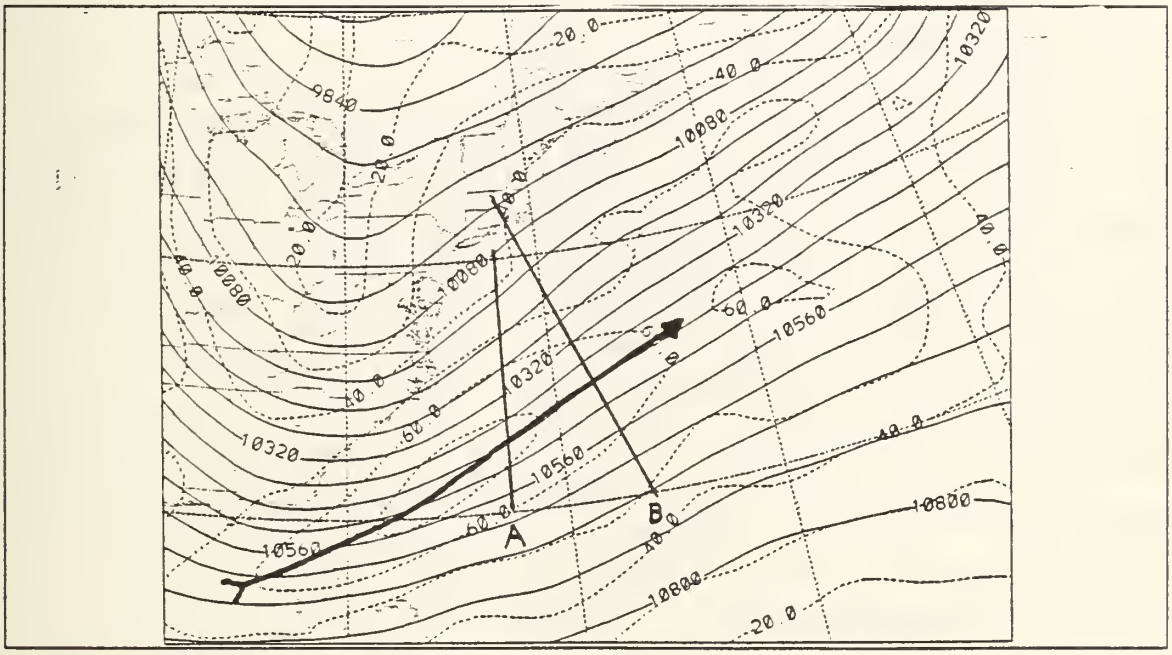

Figure 3. 0000 UTC 25 February 1986 Upper-Level Analysis: Same as Fig. 1, with jet streak highlighted. Vertical cross sections are indicated.

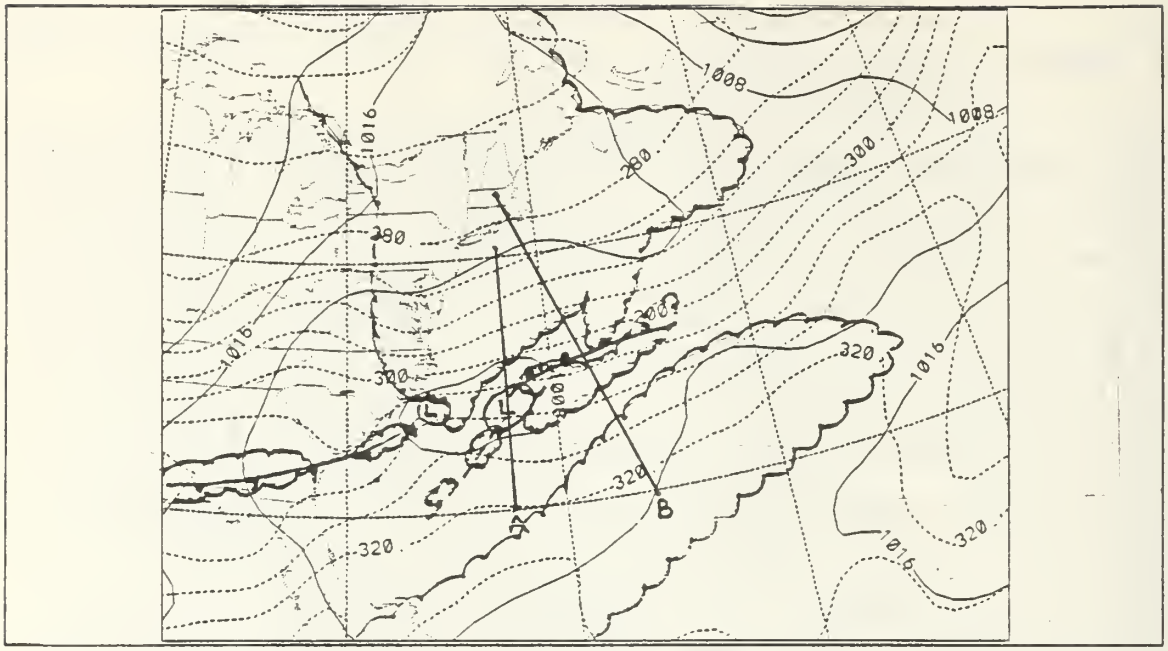

Figure 4. 0000 UTC 25 February 1986 Surface Analysis: Same as Fig. 2, with fronts and cloud outlines added.

C. 1200 UTC 25 FEBRUARY 1986

During the next 12-h, the 70-m s jet streak extended from the east coast of Florida to the east-northeast and maintained its strength and location (Fig. 5). The second jet streak continued to form downstream over the warm frontal region. The associated elongated jet structure and multiple centers complicated the vorticity advection pattern at this time, and actually reduced the PVA over the cyclone center. The NORAPS analysis of the surface pressure showed a broad low center (Fig. 6) suggestive of this complex upper-level forcing. Detailed hand analyses indicate that the low offshore deepened and moved to near 37 ° N 68 ° W along a strengthening warm front. A wave in the surface equivalent potential temperature (θ_e) analysis was present near the eastern cyclone and suggested strong coupling between this new cyclone and the intense frontal zone. GOES imagery continued to depict two distinct cloud masses; one to the south of the jet and one over the surface low.

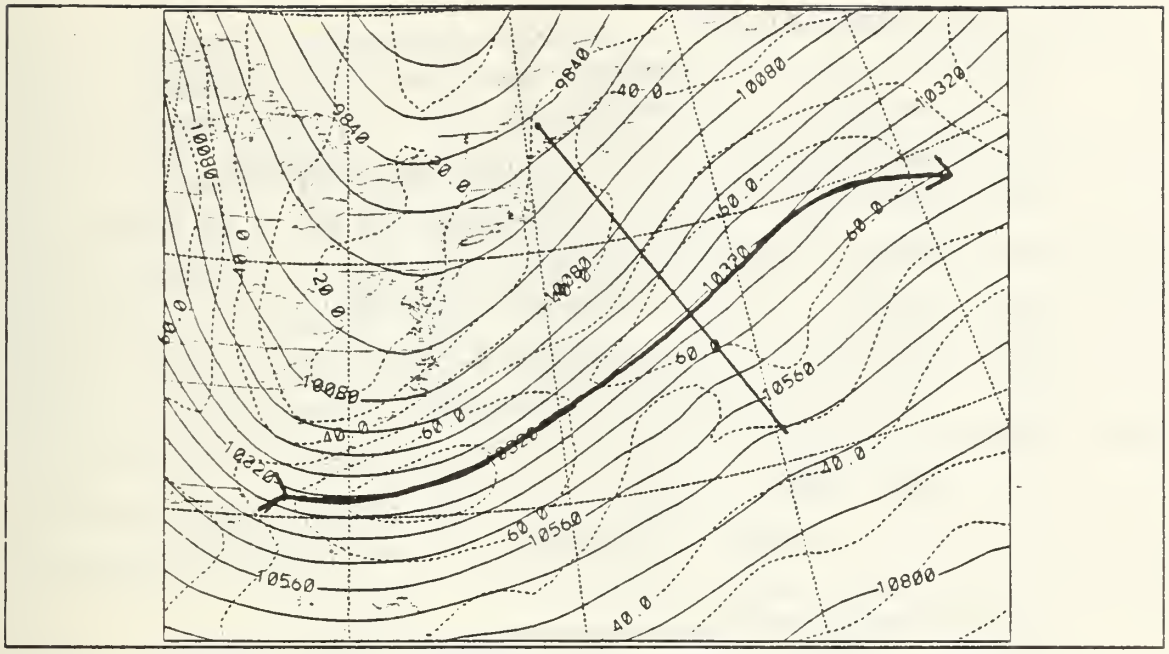

Figure 5. 1200 UTC 25 February 1986 Upper-Level Analysis: Same as Fig. 3

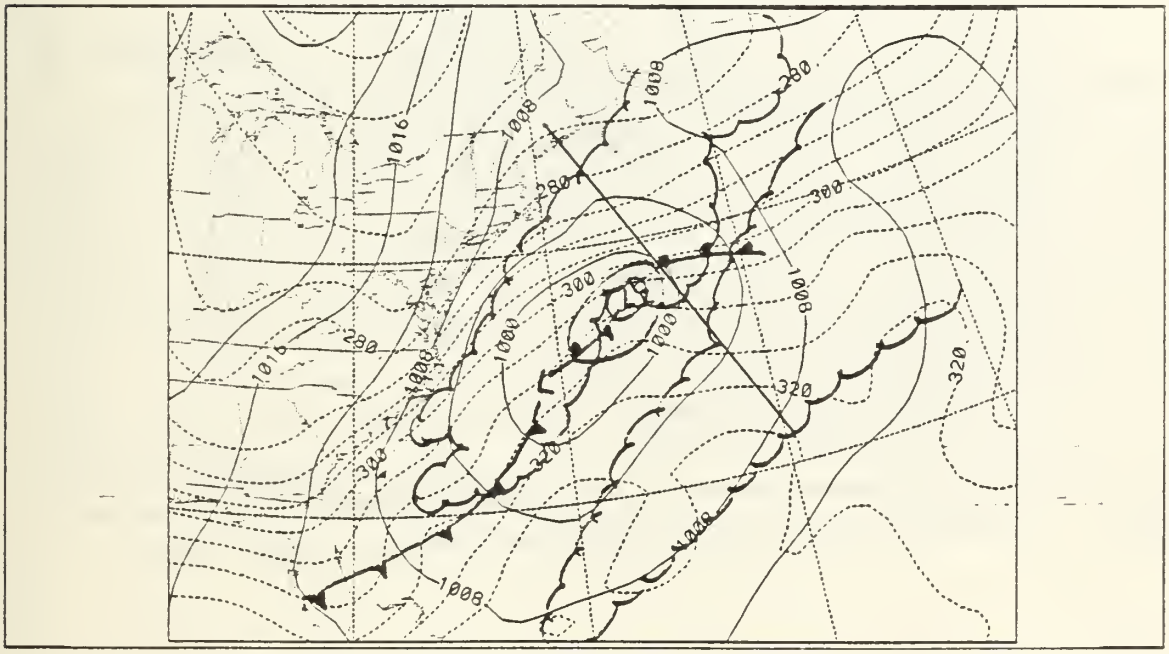

Figure 6. 1200 UTC 25 February 1986 Surface Analysis: Same as Fig. 4

D. 0000 UTC 26 FEBRUARY 1986

By this time, the downstream jet maximum strengthened considerably with a 70-m/s center at 250-mb from near 41 ° N 59 ° W to 43 ° N 56 ° W (Fig. 7). The analysis of the primary jet streak near the base of the trough indicated weakening, as did the PVA over the cyclone center. This intensity estimate is uncertain due to the difficulty of oceanic upper-air analysis. Analysis in Chapter 3 will examine the relationship of the strengthening jet south of Nova Scotia to the warm front. Despite the weaker PVA, the surface cyclone was in its explosive development stage, deepening to 980-mb. The center was analyzed at 40 ° N 63 ° W (Fig. 8). The thermal wave apparent in the θ_e analysis indicated strong surface heating ahead of the low in the ascent region and a strengthening of the front during the previous 12-h. GOES imagery suggested that the separate cloud features previously observed had combined into a more unified cloud feature to the east and northeast of the cyclone.

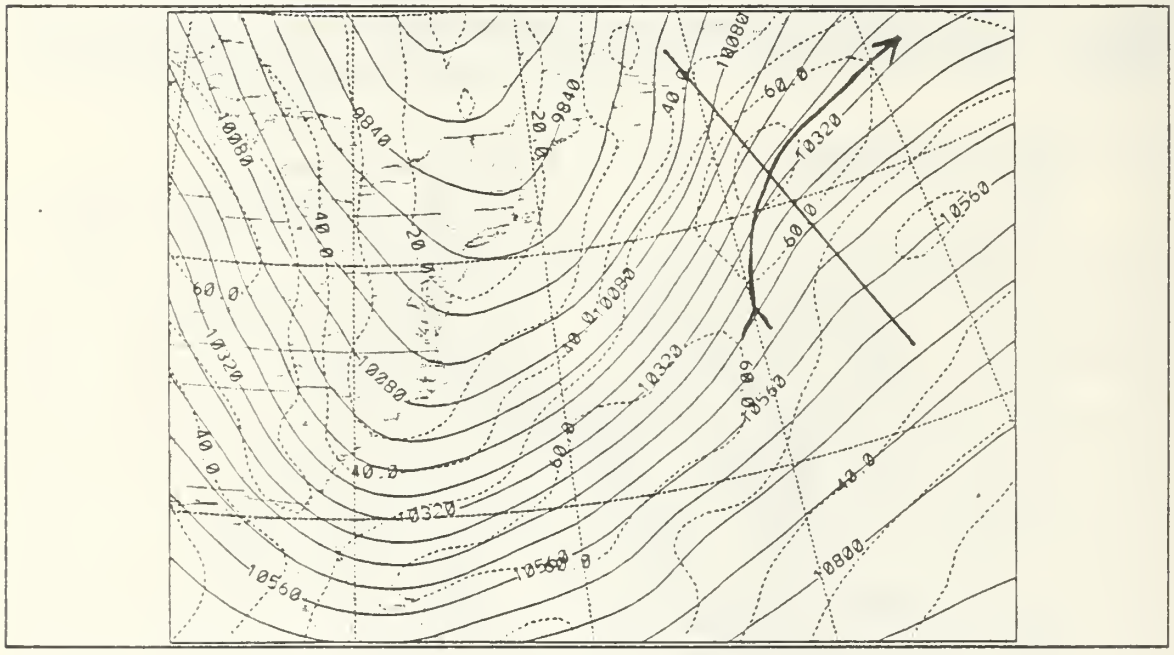

Figure 7. 0000 UTC 26 February 1986 Upper-Level Analysis: Same as Fig. 3

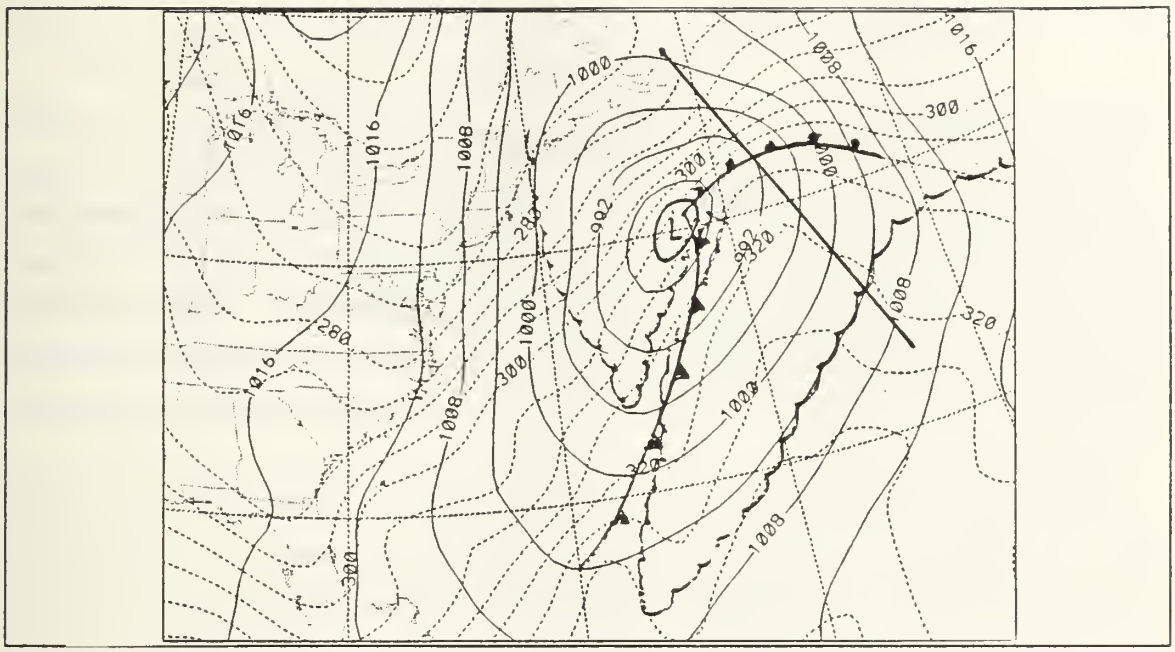

Figure 8. 0000 UTC 26 February 1986 Surface Analysis: Same as Fig. 4

E. SUMMARY

In summary, the interesting synoptic aspects of IOP9 are the upper-level jet behavior and the surface structure. Two distinct 250-mb jet streaks dominated the upper-level pattern. The upstream jet streak dominated the pattern early in the period. At 1200 UTC 25 February, the downstream streak increased in size. 12-h later, this jet streak intensified and the upstream jet streak apparently weakened. Two surface low pressure centers were present early in the period, but the coastal low moved offshore and weakened. The second cyclone center moved to the northeast and deepened along a strong warm front. At 0000 UTC 26 February its deepening rate of 12-mb in 12-h met the criteria for explosive development.

III. RESULTS

A. SYMMETRIC STABILITY AHEAD OF THE CYCLONE IN IOP9

Symmetric instability is a type of convective instability that can occur in baroclinic flow. Instability results from an imbalance of body forces acting on a fluid. If the responsible force is gravitational, the instability will be convective. If the force is centrifugal, the instability will be inertial. Convective and inertial instabilities differ in the direction in which the restoring forces act; gravitational forces act in the vertical, and centrifugal forces act radially.

Symmetric instability results from a combination of vertical and radial restoring forces. The motion resulting from convective instability is vertical; such convection is referred to as "upright". The motion resulting from symmetric instability includes a radial component; this convection is referred to as "slantwise". The atmosphere can be stable to upright convection but still produce significant convective development. Bennetts and Hoskins (1979) and Emanuel (1983) have suggested that such development may be slantwise convection driven by symmetric instability.

Emanuel (1983) demonstrated that slantwise convection is on a small enough-scale to treat with parcel theory. In the case of slantwise convection, the parcel is lifted slantwise instead of vertically. In addition to conserving its potential temperature, θ, the parcel also conserves its pseudo-absolute momentum, defined as $M = v + fx$, where v is the geostrophic thermal wind, and x is the coordinate perpendicular to the thermal wind.

Potential vorticity, q, can be defined by $-\eta \frac{(\partial\theta)}{(\partial p)}$, where η is absolute vorticity on potential temperature surfaces. Moist potential vorticity, q_w, is defined using equivalent potential temperature, θ_e. In a moist symmetrically neutral atmosphere, a parcel lifted along a constant M surface will conserve θ_e and q_w will become zero. Solutions of the Sawyer-Eliassen equation derived by Emanuel (1985) indicate strong response to frontogenesis in regions where moist potential vorticity vanishes. In the numerical simulations, a strong, small-scale updraft occurred on the warm side of the maximum isotherm gradient. Sanders (1986b) offered observational evidence that small symmetric stability in the warm air ahead of a cyclone, accompanied by frontogenetical forcing, forced the ascent. It will be shown that symmetric neutrality occurred in the warm

frontal region ahead of the cyclone in IOP9, where surface frontogenesis forced a strong updraft.

Two different methods have been developed to evaluate symmetric stability (Sanders, 1986b). The first method involves the construction of vertical cross sections oriented parallel to the mean temperature gradient throughout the troposphere. Absolute momentum, M, is analyzed in the cross section, as well as θ for an unsaturated atmosphere or θ_e for a saturated atmosphere. Using the thermal wind relation and geostrophy, Sanders (1986b) showed that symmetric instability is present if the θ or θ_e surfaces are more steeply sloped than the M surfaces. Parallel surfaces of θ or θ_e and M indicates symmetric neutrality.

Even with the enhanced GALE data network, the region of active frontogenesis in IOP9 was in a data sparse area. The special dropwinsondes were not in position to construct cross sections across the warm front ahead of the cyclone. Instead, gridded data were used to analyze the θ, θ_e and M surfaces. Since moisture fields are 12-h forecasts from the model, the cross-sectional θ_e analyses are only estimates (hopefully representative) of the actual moisure distribution. Cloud outlines from GOES imagery were hand-drawn on the cross sections to indicate areas where the atmosphere was saturated. Cloud-top temperatures from the GOES images were used to determine the depth of the clouds. Reed and Albright (1986) used a similar technique based on the theory that in cloudy regions θ_e surfaces should be nearly vertical. An Omega dropwinsonde was dropped by a Citation aircraft flown by the National Oceanic and Atmospheric Administration (NOAA) for the GALE experiment at 0400 UTC 25 February 1986. Although the sounding could not be used to construct a cross section, the cross-sectional analysis from the gridded data was supported by θ_e values calculated from the sounding. The orientation of the cross section is indicated as "A" in Fig. 3. The results, shown in Fig. 9, indicate that the θ_e surfaces were much steeper (more vertical) than the M surfaces in the cloudy regions near this point. In fact, the gridded data indicated potential unstability in the 850-700-mb layer on the south half of the cross section. Hence, the gridded θ_e analysis appears to successfully identify critical moist dynamic regions for this time period.

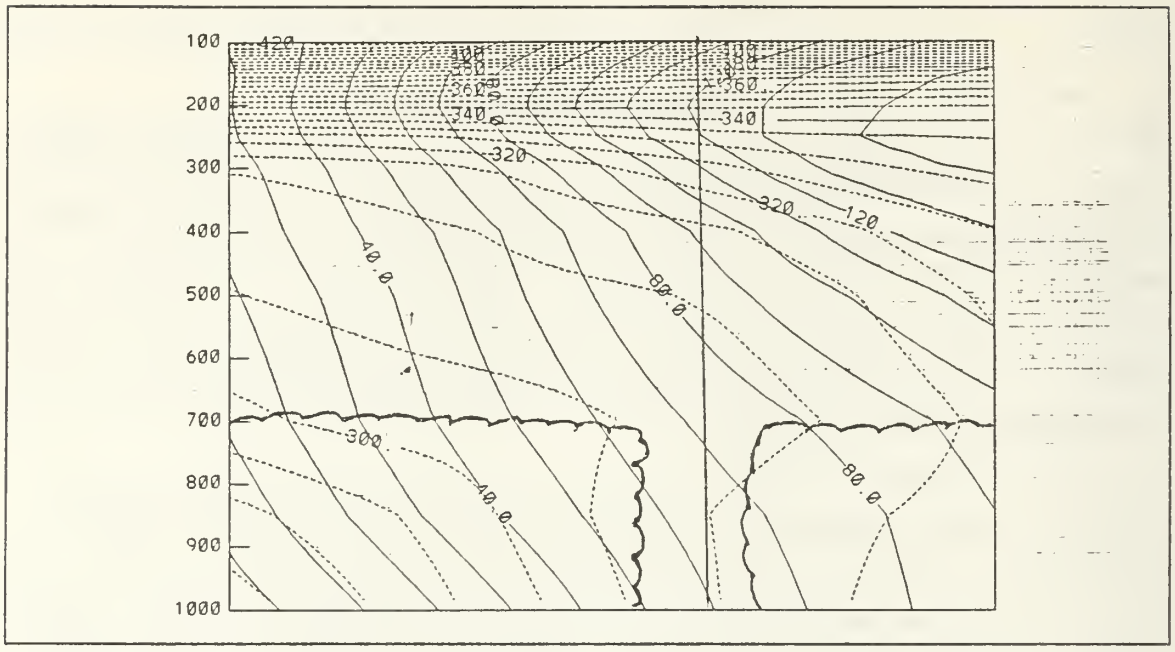

Figure 9. Cross section of M and θ_e: Solid lines are M in-m/s; dashed lines are θ_e in K. Cross section is indicated on Fig. 3.

To check this result, a procedure developed by Emanuel (1983) to assess symmetric stability from a single atmospheric sounding was applied to the 0400 UTC dropwinsonde. Upright convective instability is evaluated on a sounding by lifting a parcel along its dry adiabat until saturated, then continuing along a moist adiabat. The parcel temperature is compared to its environment throughout the depth of the layer being evaluated. If the parcel temperature, T_p, is greater than the environmental temperature, T, the parcel will continue to rise, and the atmosphere is unstable to upright convection. If T_p is less than T, the parcel will return to its original position, and the atmosphere is stable to upright convection. In a neutral case, T_p is equal to T, and the parcel will not move.

Symmetric or slantwise convective instability is evaluated by lifting a parcel along a surface of constant M. On a sounding, the value

$$\frac{1}{2}\,\frac{T_0}{g}\,\frac{f}{\eta}\,\frac{(v_{z1}-v_{z2})^2}{(z_2-z_1)} \tag{1}$$

is added to the parcel temperature at each level. Here, T_0 is the surface equivalent potential temperature, $(v_{z1}-v_{z2})$ represents the magnitude of the thermal wind, and

$(z_2 - z_1)$ is the thickness of the layer being considered. This adjusted parcel temperature is equivalent to the temperature a parcel would have if lifted in such a way that it conserves both M and θ values. The adjusted parcel temperature is then compared to its environment at each level. Stability is evaluated using the same criteria as in the case of upright convection.

The 0400 UTC Omega dropwinsonde was located at 33.7 ° N 72.8 ° W, just ahead of the surface cyclone. The location of the sounding is indicated on the cross section in Fig. 9. Although the sounding location was in a clear region on the 0000 UTC analysis, it shows that clouds were probably present at 0400 UTC. (Fig. 10). The sounding was evaluated for symmetric stability using the procedure described above. The sounding was conditionally unstable to upright convection from the surface to about 700-mb. The adjusted parcel temperature was nearly equal to the environmental temperature up to about 700-mb, indicating slantwise convective neutrality. Above 700-mb, the adjusted parcel temperature was slightly cooler than the environment, indicating a change to small slantwise convective stability. This single sounding evaluation agreed with the gridded cross section which showed increasing slantwise stability above 700-mb.

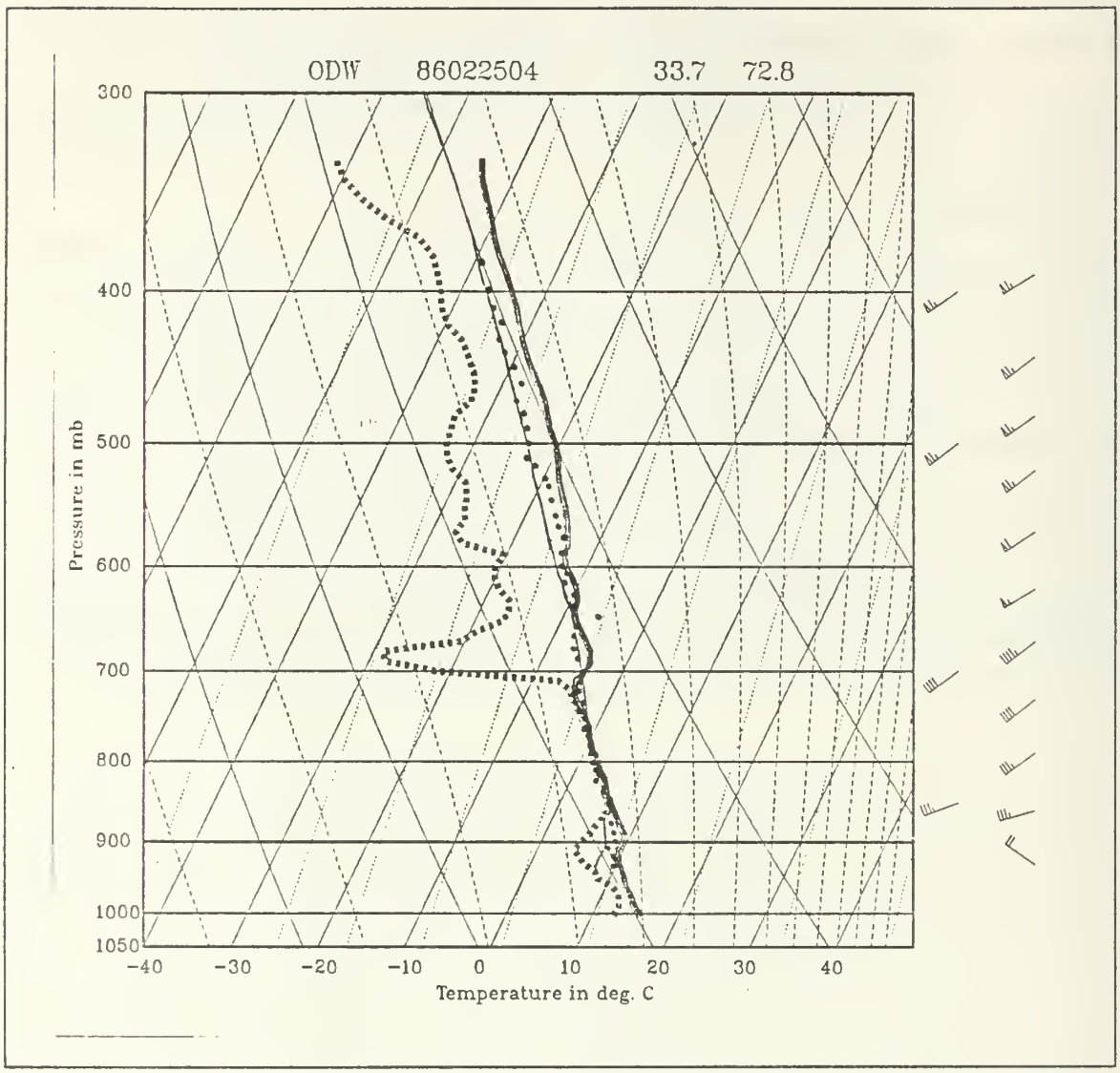

Figure 10. Omega dropwinsonde, 0400 UTC 25 February 1986: Solid line is temp sounding; dots represent adjusted parcel temp

Although the dropwinsonde was located along the cross section, it was not used directly in the construction of the M and θ_e surfaces. The cross section was constructed from gridded analyses with the NORAPS 80-km grid resolution. Consequently, small-scale details of the analyzed surfaces were smoothed. Since the sounding indicated symmetric neutrality in the cloud region, it seems reasonable to expect that a cross section constructed from several actual soundings would depict θ_e surfaces nearly parallel to the M surfaces through the cloud region.

Symmetric neutrality can be inferred from any cross section with good θ_e and M analyses. Since there were no soundings available in the critical warm frontal region ahead of the cyclone in IOP9, the cross section method was used to assess symmetric neutrality from the gridded data. The orientation of the cross sections studied are indicated on Fig's 3, 5 and 7. At 0000 UTC 25 February, cross section "B" showed the PBL was convectively unstable (Fig. 11). A shallow region of symmetric instability existed along the warm front. South of the jet streak, a large region of symmetric neutrality instability was indicated on the right side of Fig. 11 up to 300-mb. This region corresponded well with the deep clouds present on the GOES imagery. The deep clouds on the left side of Fig. 11, where the atmosphere was symmetrically stable, were associated with ascending air under the left exit region of the upstream 250-mb jet streak.

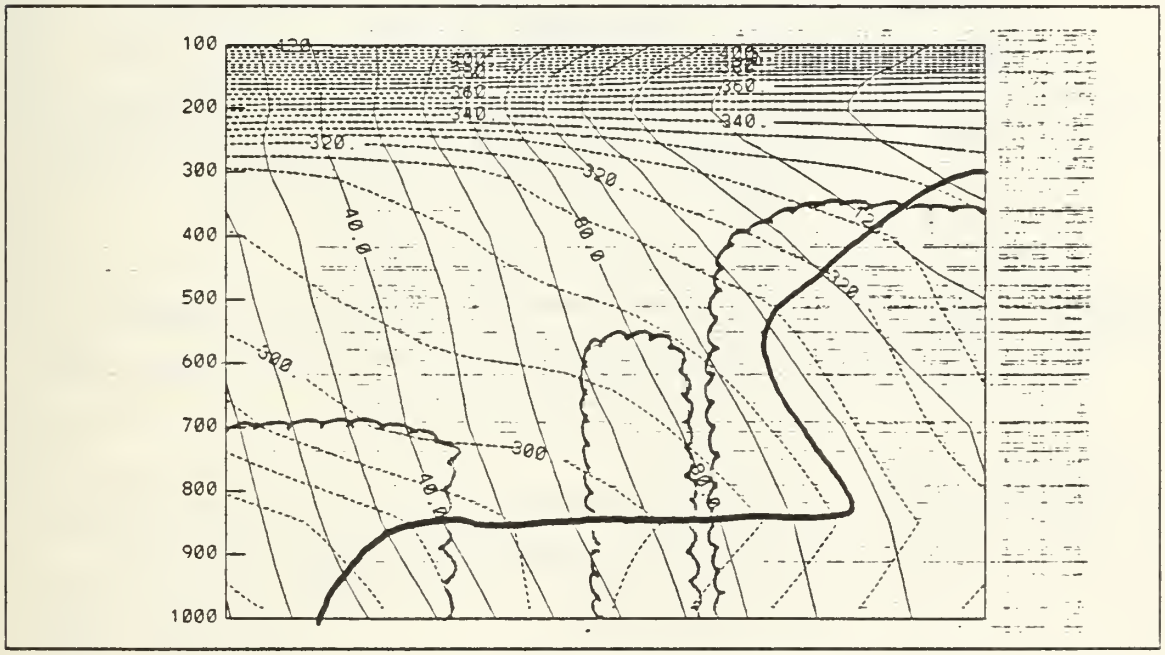

Figure 11. **0000 UTC 25 February 1986 Cross section of M and θ_e:** M, m/s (solid) and θ_e, K (dashed). Cloud outline added. Area within heavy solid line is symmetrically neutral or unstable. Location of cross section indicated as "B" on Fig. 3.

At 1200 UTC, the layer of symmetric neutrality near the warm front deepened and encompassed the cloud region, as seen in the cross section through the entrance region of the jet streak (Fig. 12). The region of symmetric neutrality instability persisted aloft

on the right side of the jet. Again the GOES imagery indicated deep cloudiness in this region. The symmetrically stable region on the left side of Fig. 12 was under the left entrance region of the 250-mb downstream jet streak and represents the stable lifting associated with the trough. GOES imagery indicated a solid area of low and middle clouds in this stable region.

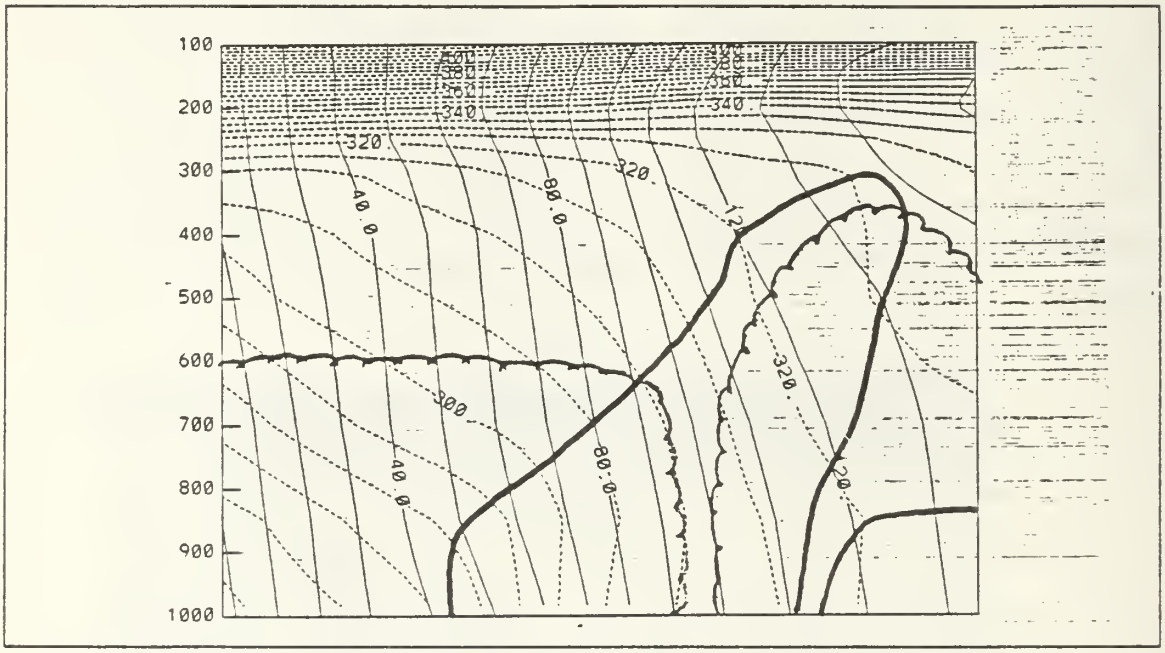

Figure 12. 1200 UTC 25 February 1986 Cross section of M and θ_e: Same as Fig. 11 Location of cross section indicated in Fig. 5.

At 0000 UTC 26 February, the cross section across the center of the jet showed one narrow region of symmetric neutrality that extended from the surface warm front up to 300-mb. (Fig. 13). This region extended across to the warm side of the jet in the 300-400-mb layer, where the deep clouds south of the jet were previously found. The GOES imagery indicated a unified cloud mass with cloud-tops near the tropopause.

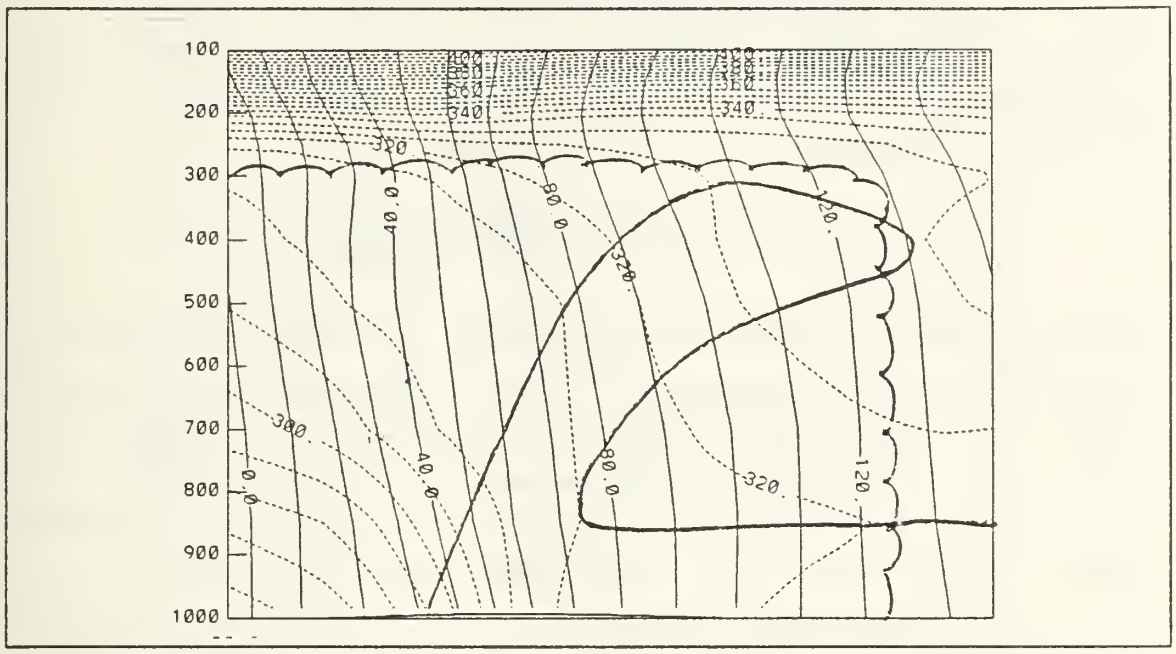

Figure 13. 0000 UTC 26 February 1986 Cross section of M and θ_e: Same as Fig. 11 Location of cross section indicated in Fig. 7.

In summary, deep regions of symmetric neutrality/instability existed at all time periods. At 0000 UTC 25 February, the deep region was well south of the warm front, associated with the clouds on the anticyclonic side of the jet. As time progressed, the symmetric neutrality/instability extended from the surface warm front through a progressively deeper layer of the atmosphere. Throughout the period, extensive cloudiness was present in the symmetrically stable regions that can be associated with the primary upper-level trough.

B. INCREASES IN SURFACE EQUIVALENT POTENTIAL TEMPERATURE

Hoskins et al. (1985) suggested that surface θ_e and moist potential vorticity, q_m, throughout the atmosphere determine the synoptic-scale dynamics for a moist baroclinic cyclone. As previously stated, the warm frontal region ahead of a cyclone exists in an atmosphere of moist symmetric neutrality, where q_m goes to zero and it may in fact be slantwise or vertically convectively unstable. Therefore, in the vicinity of the warm front ahead of the cyclone, changes in surface θ_e represent a strong thermodynamic contribution to the development of the cyclone.

The two primary processes responsible for changes in the surface θ_e are advection, and surface heat and moisture fluxes. To determine which process contributed to increasing surface θ_e in the vicinity of the warm front, the planetary boundary layer (PBL) θ_e tendency was computed using the following equation:

$$\frac{(\partial \theta_e)}{(\partial t)} = -\vec{V} \cdot \nabla \theta_e - \overline{w} \frac{(\partial \theta_e)}{(\partial z)} - \frac{\partial (\overline{w'\theta'_e})}{(\partial z)} . \qquad (2)$$

The first two terms on the right represent horizontal and vertical advection of θ_e. The last term represents the flux divergence of θ_e, which is approximated by the surface flux divided by the height of the boundary layer top (assumed to be 850-mb), where entrainment flux is assumed to be zero. Boundary later heat and moisture fluxes were computed using the PBL model of Brown and Liu (1982) applied to the NORAPS gridded data. The model uses a modified Ekman solution to relate surface wind and fluxes to the 850-mb wind. Sea-surface temperature (SST) was analyzed from climatology rather than actual data, so horizontal SST gradients were smoothed.

At 0000 UTC 25 February, the PBL analysis indicated a maximum θ_e increase of 40 K/day ahead of the cyclone south of the warm front (Fig. 14). An increase of 30-40 K/day is a typical θ_e change for a vigorous oceanic cyclone (Nuss and Kamikawa, 1988). This increase was located in a shallow region of symmetric neutrality, as was seen in Fig. 11. The deepest region of symmetric neutrality/instability lies just south of the maximum θ_e increase. Separating (2) into its components and plotting each term individually isolates the contribution of each term to the total. As shown in Fig. 15 the horizontal advection of θ_e accounted for more than half of the total increase and the flux divergence term (Fig. 16) provided the rest of the increase. The vertical advection term (not shown) was near zero. Analyses of the actual flux terms indicated a maximum heat flux of more than 30 W/m^2 (Fig. 17) and a moisture flux of more than 180 W/m^2 (Fig. 18) in the region of maximum θ_e increase. Other notable features revealed in the flux computations included two strong maxima along the coast, one off Maryland and the other off northeastern Florida. The first area, north of the surface cyclone, showed a maximum heat flux of greater than 90 W/m^2 and a moisture flux of greater than 210 W/m^2. The stronger area along the Florida coast showed a heat flux of 120 W/m^2 and a moisture flux of 480 W/m^2.

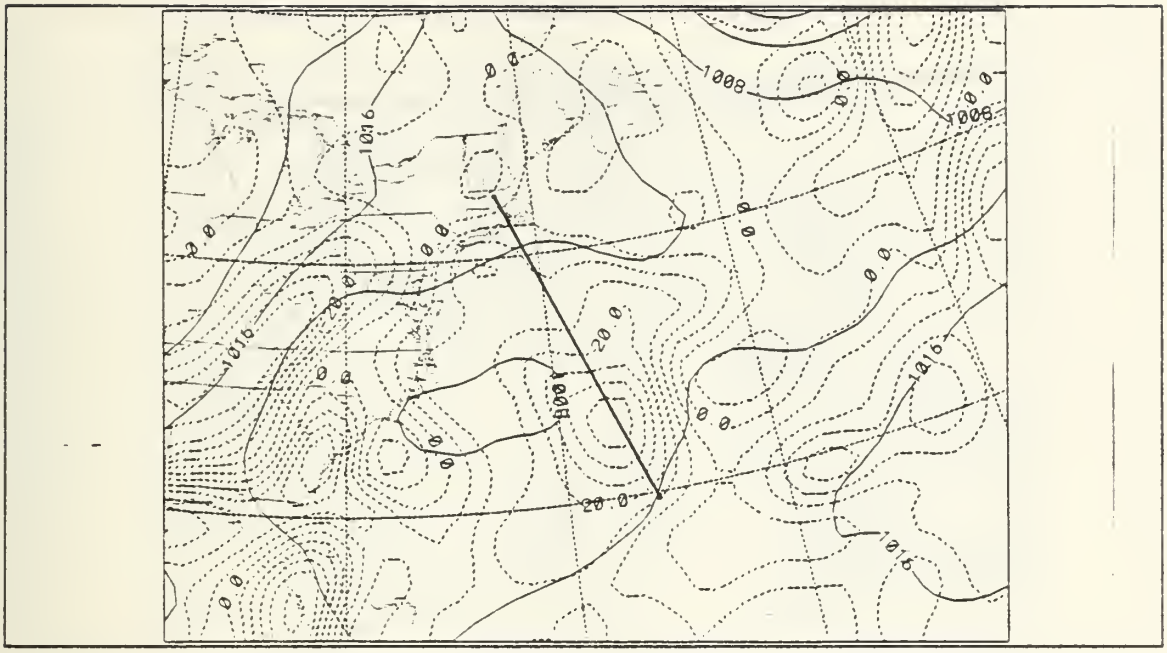

Figure 14. 0000 UTC 25 February 1986 Total increase in θ_e: in K/day. Solid lines are sea level pressure in mb.

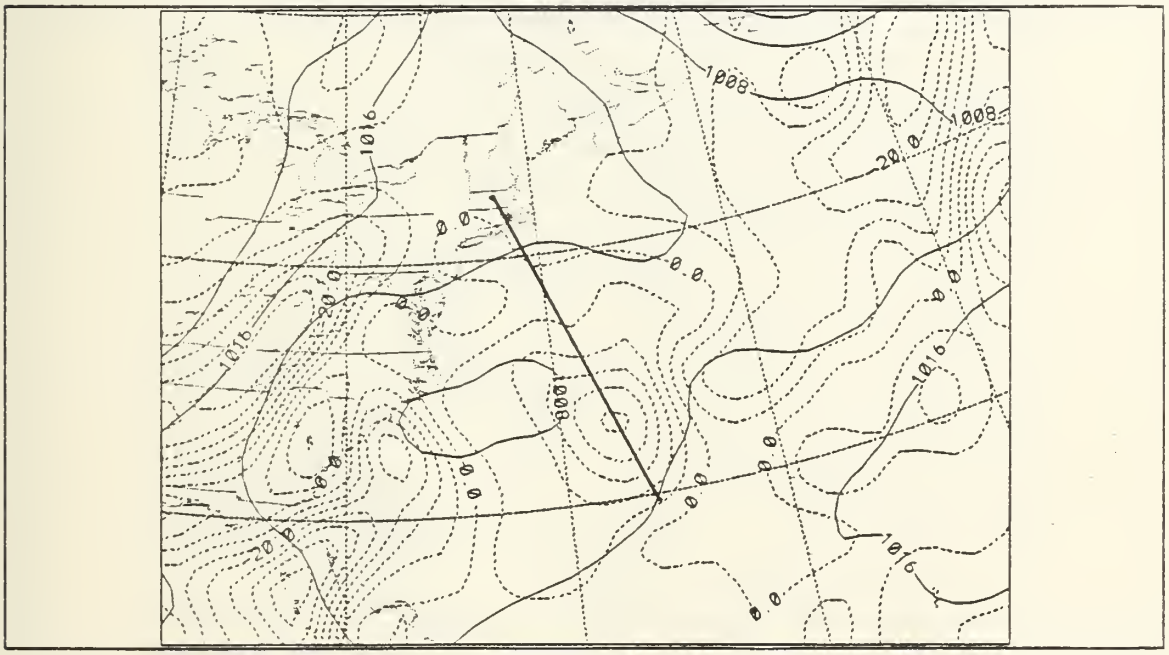

Figure 15. 0000 UTC 25 February 1986 Horizontal advection of θ_e: in K/day. Solid lines are sea-level pressure in mb.

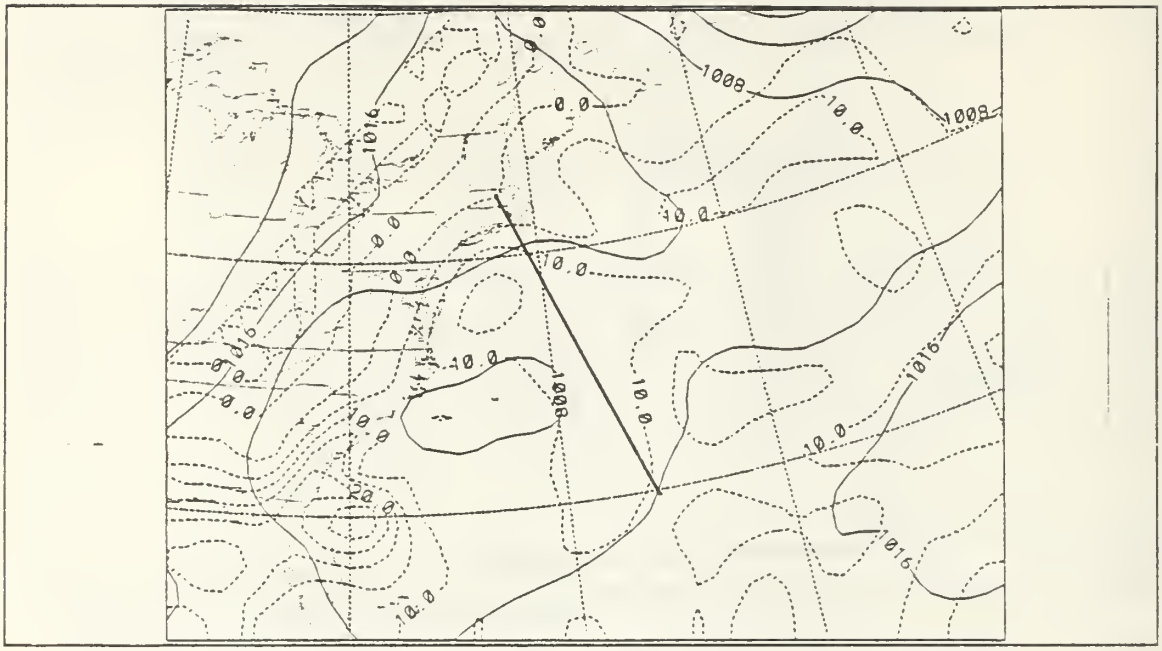

Figure 16. 0000 UTC 25 February 1986 Flux divergence term: in K day. Solid lines are sea-level pressure in mb.

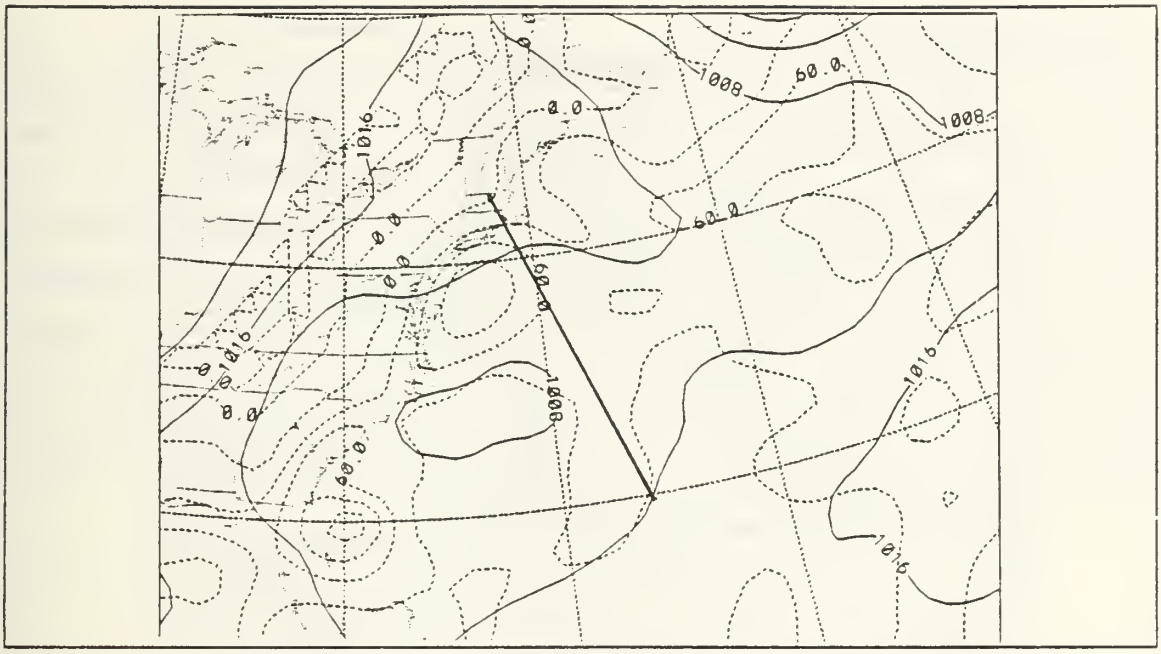

Figure 17. 0000 UTC 25 February 1986 Surface heat flux: in W/m^2. Solid lines are sea-level pressure in mb.

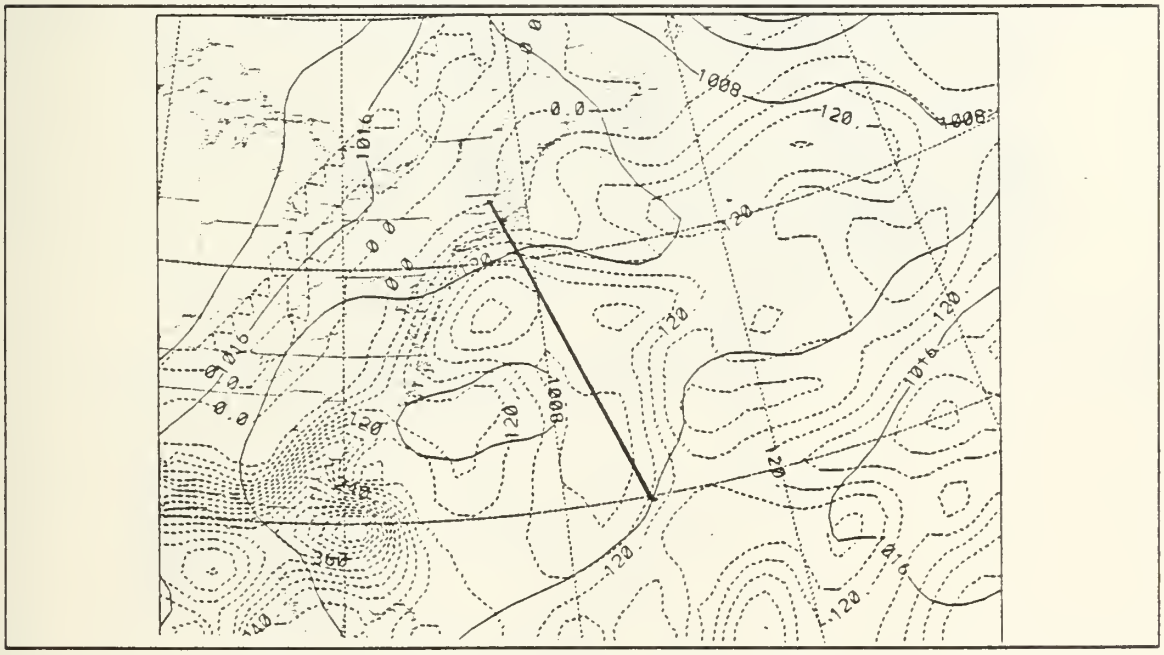

Figure 18. 0000 UTC 25 February 1986 Surface moisture flux: in W/m^2. Solid lines are sea-level pressure in mb.

By 1200 UTC 25 February, horizontal advection was responsible for approximately 70 percent of the total increase in θ_e. At this time, the maximum θ_e increase of 65 K/day (Fig. 19) was located further ahead of the deepening cyclone on the warm front. As was seen in Fig. 12, a deep, sloping region of symmetric neutrality/instability existed on the warm front. The maximum θ_e increase on the cross section was on the warm front, with a magnitude of 50 K/day. The horizontal advection term (Fig. 20) was stronger at this time in response to increasing surface flow. Again the vertical advection term (not shown) was near zero. Flux divergence (Fig. 21) accounted for more than a 20 K/day increase in θ_e. The surface heat flux at this time was still 30 W/m^2, but the surface moisture flux increased to more than 240 W/m^2 (not shown).

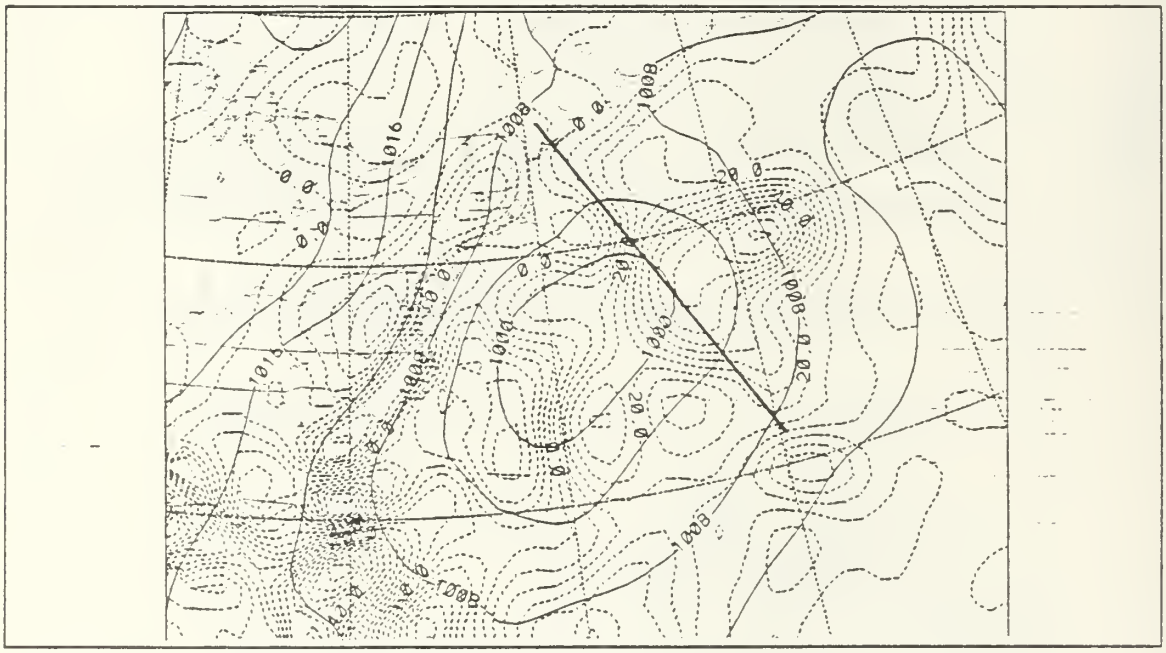

Figure 19. 1200 UTC 25 February 1986 Total increase in θ_e: Same as Fig. 14

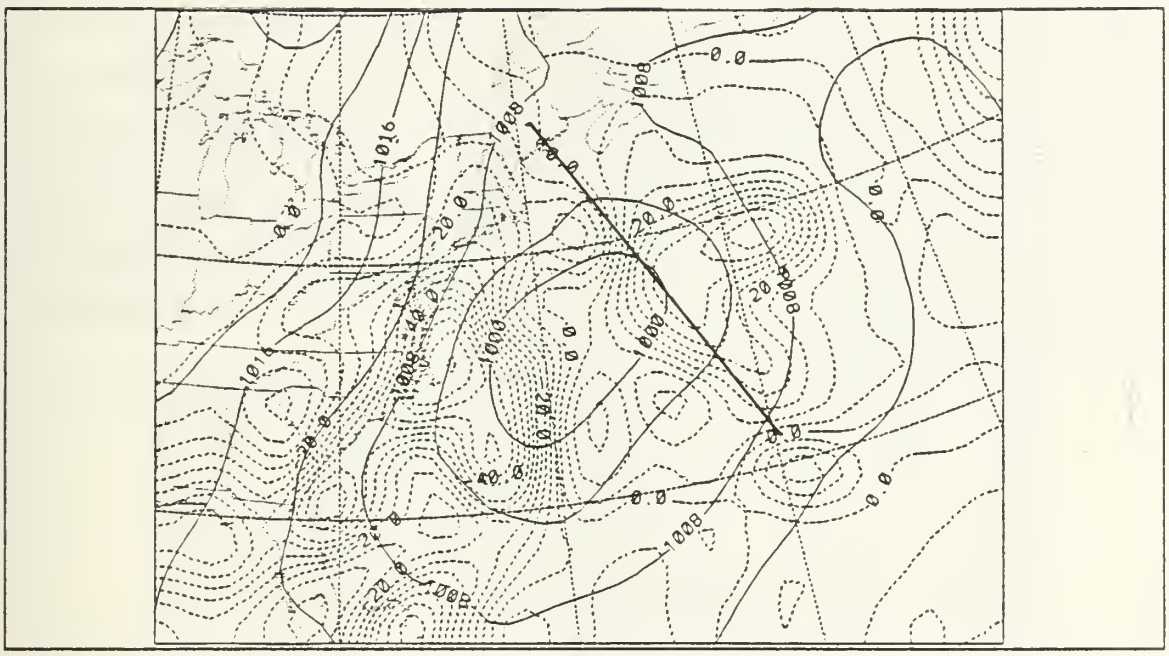

Figure 20. 1200 UTC 25 February 1986 Horizontal advection of θ_e: Same as Fig. 15

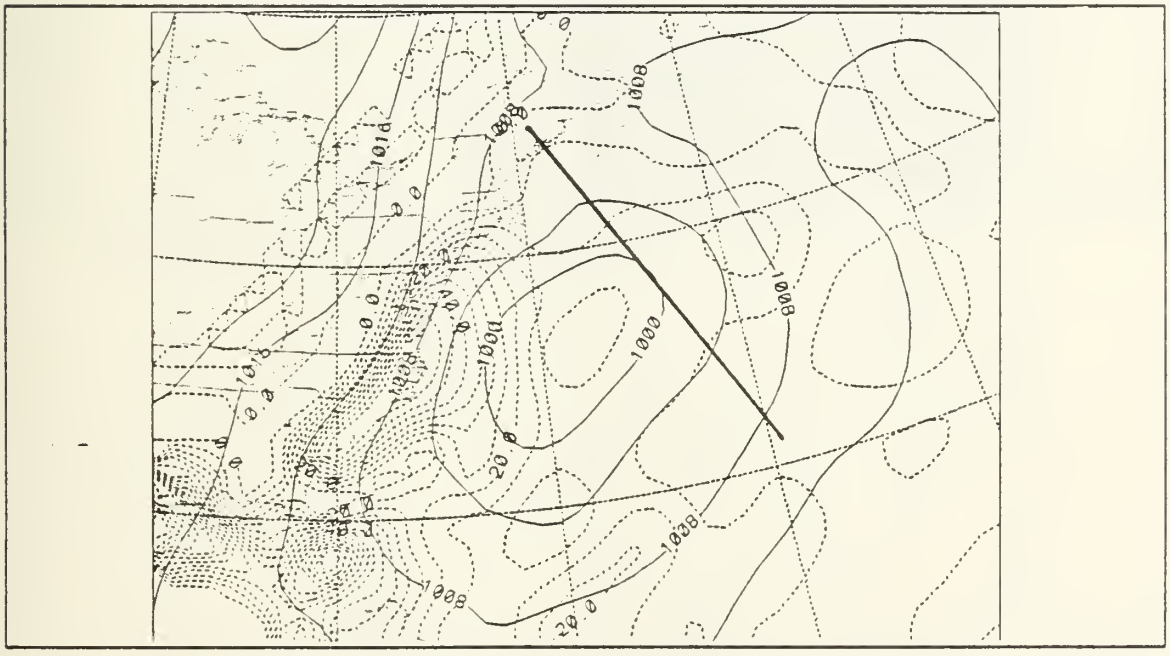

Figure 21. 1200 UTC 25 February 1986 Flux divergence term: Same as Fig. 16

By 0000 UTC 26 February, the surface cyclone was deepening explosively. The total PBL budget (Fig. 22) showed an increase in θ_e of 65 K day in the region ahead of the warm front. The maximum θ_e increase on the cross was on the warm front, coincident with the deep region of symmetric neutrality/instability shown in Fig. 13. Horizontal advection increased θ_e by 85 K/day (Fig. 23), but vertical advection in the updraft region decreased θ_e by 25 K/day, as shown in (Fig. 24) The flux divergence term decreased θ_e by 5 K/day, as shown in Fig. 25.The surface heat flux was downward in this region and the moisture flux (not shown) was slightly negative.

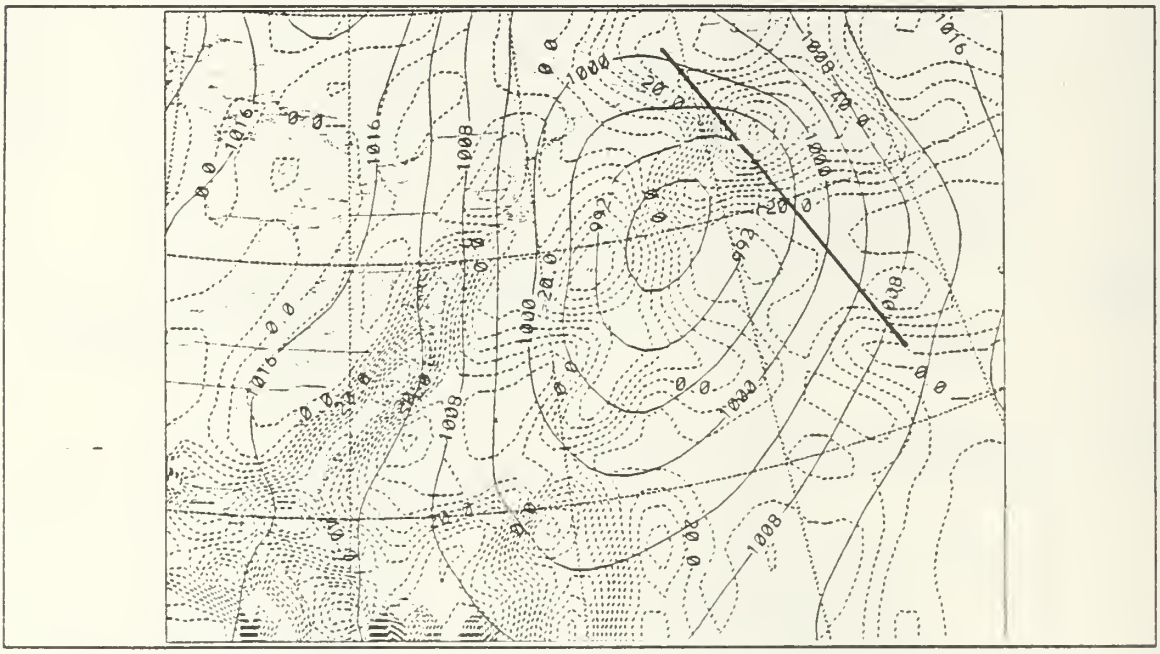

Figure 22. 0000 UTC 26 February 1986 Total increase in θ_e: Same as Fig. 14

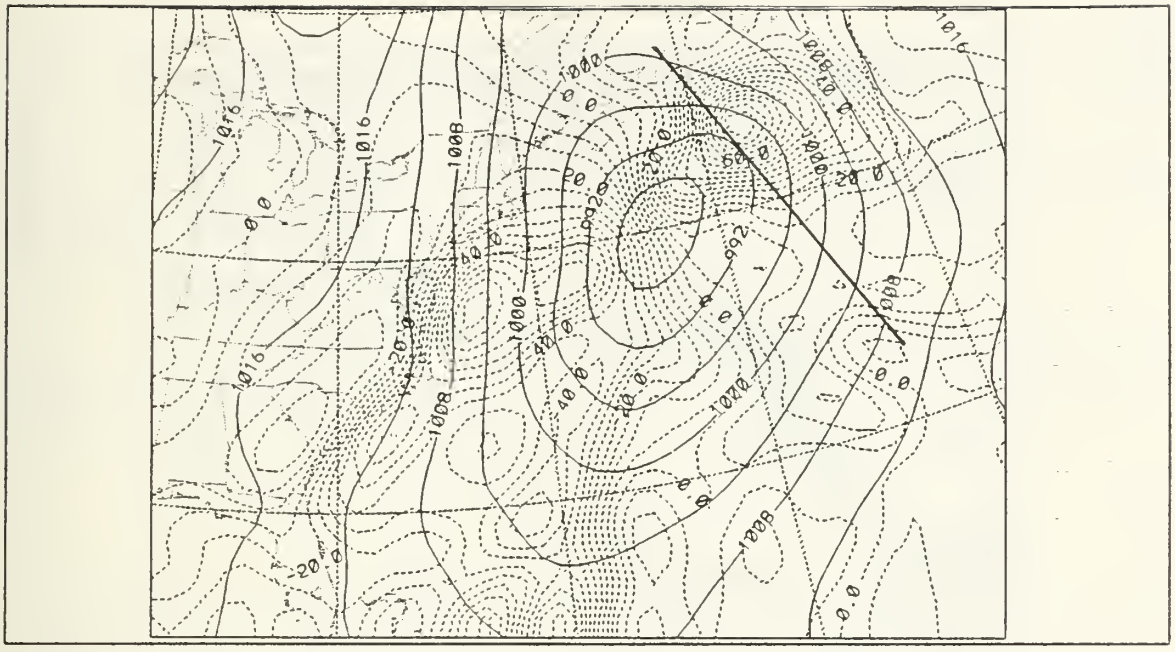

Figure 23. 0000 UTC 26 February 1986 Horizontal advection of θ_e .: Same as Fig. 15

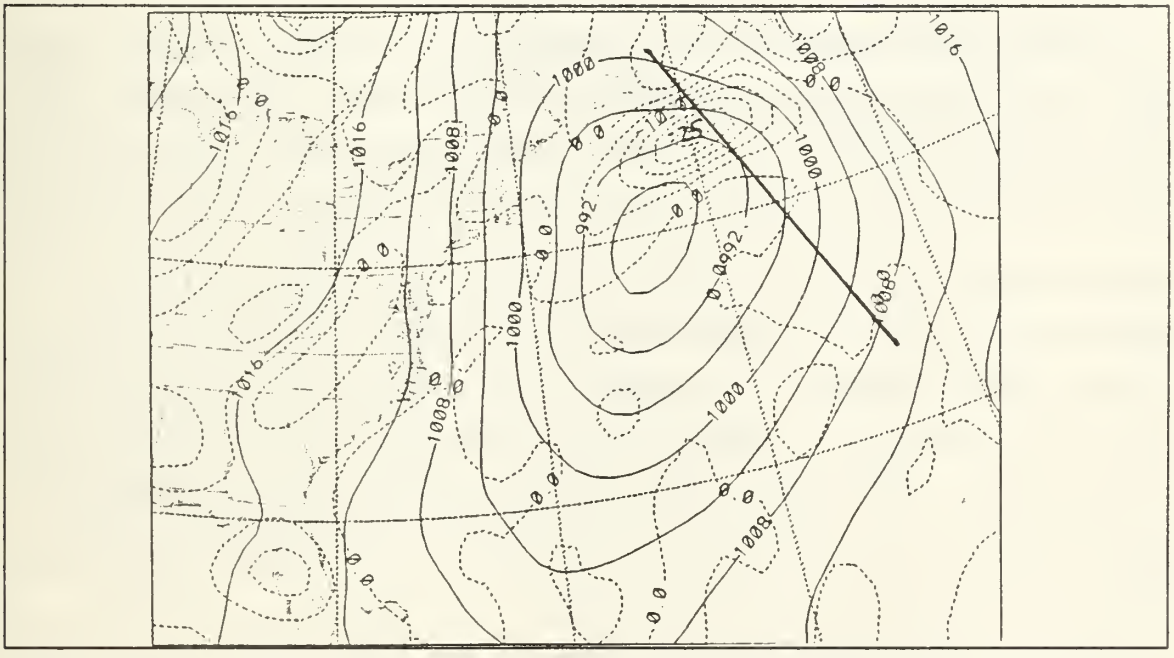

Figure 24. 0000 UTC 26 February 1986 Vertical advection of θ_e .: in K/day. Solid lines are sea-level pressure in mb.

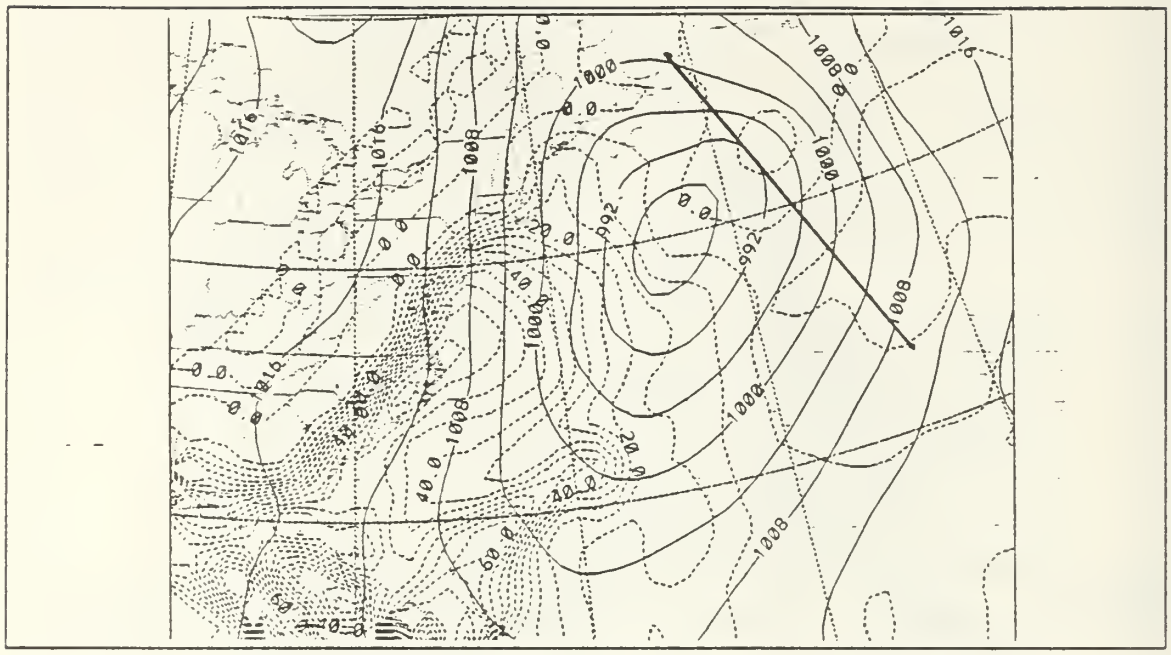

Figure 25. 0000 UTC 26 February 1986 Flux divergence term: Same as Fig. 16

Throughout the development of the surface cyclone, horizontal advection was the dominant mechanism that increased surface θ_e in the updraft region. During the period of rapid deepening, the horizontal advection term was strong enough to overcome a strong decrease in θ_e caused by vertical advection. Flux divergence accounted for nearly half of the θ_e increase early in the development but contributed little as the surface cyclone moved over colder water and the surface fluxes became negative. The importance of surface fluxes to the early developoment of the cyclone in IOP9 contradicts classic quasi-geostrophic theory of cyclogenesis, where horizontal and vertical advection are the primary processes that amplify the baroclinic wave (Holton, 1979). The strong northward advection of θ_e supplemented by significant surface fluxes which warmed and moistened the PBL were responsible for the weak symmetric instability regions shown on Fig.'s 9,11,12 and 13.

C. FORCING MECHANISMS IN THE UPDRAFT REGION

It has been established that the boundary layer in the region ahead of the cyclone was heated and moistened by surface fluxes and by advection of θ_e into the region. Since the atmosphere near the warm front was symmetrically neutral, a surface increase in θ_e

must be compensated by a θ_e increase aloft. The upper-level θ_e increase was presumably accomplished by slantwise convective adjustment (Emanuel, 1988) in the updraft region. To understand the importance of the surface processes in this case, the upper and low-level forcing mechanisms of the updraft have been examined. One source of upper-level forcing was divergence associated with the jet streak. Low-level forcing was provided by surface frontogenesis.

1. Subtropical Jet

The vorticity and divergence patterns associated with jet streaks induce vertical circulations and play an important role in surface cyclogenesis. For straight flow, the vorticity equation can be approximated by:

$$\vec{V} \cdot \nabla \eta \simeq - \eta \nabla \cdot \vec{V}. \tag{3}$$

The advection of vorticity and divergence are in approximate balance by neglecting the contributions from the vertical advection, local tendency and tilting terms. In the absence of curvature effects, vorticity will be entirely due to shear effects. In the northern hemisphere, the maximum cyclonic vorticity will occur on the left side of the jet maximum and the minimum cyclonic vorticity will occur on the right side. Maximum cyclonic or positive vorticity advection will thus occur in the right entrance region and left exit region of the jet streak. From the above equation, regions of maximum positive vorticity advection also will be regions of maximum divergence at jet level. By mass continuity, regions of horizontal divergence must have compensating ascent below the jet. Thus, the left exit and right entrance regions of jet streaks in straight flow will be regions of upward vertical motion.

As shown in Fig. 3 at 0000 UTC 25 February, a 70-m/s jet streak at 250-mb extended from off the east coast of Florida northeastward. The left exit region of the jet streak was ahead of the offshore surface cyclone center on the warm front. A cross sectional analysis of wind, θ_e and ageostrophic circulation taken through the exit region (Fig. 26) indicated a strong updraft associated with the left exit region. This is consistent with classic ideas of oceanic cyclogenesis. In a study of two cases of explosively developing cyclones, Wash et al. (1988) concluded that rapid deepening occurred because of the singular favorable location of the upper-level jet streak with respect to the surface cyclone. At this time, the updraft region was symmetrically neutral/unstable only in the PBL region.

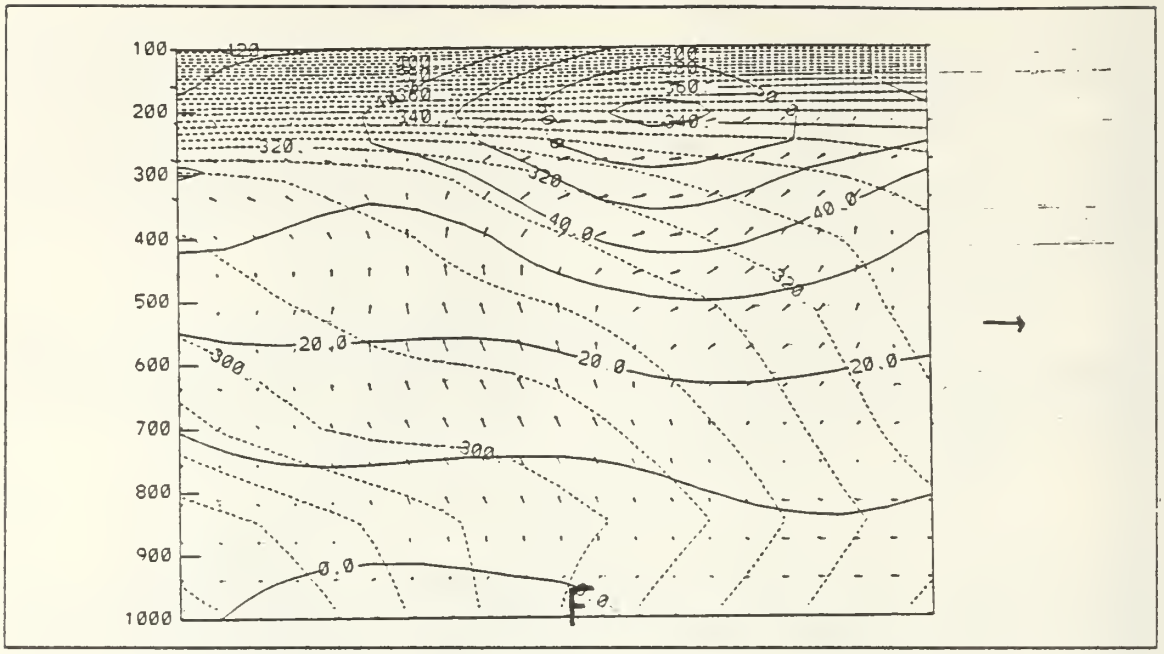

Figure 26. 0000 UTC 25 February 1986 Cross section of isotachs and θ_e: Isotachs in m/s (solid) and θ_e in K (dashed). Arrows are ageostrophic flow, with maximum vector to right of figure 20-m/s. Surface frontal location indicated by F. Location of cross section indicated in Fig. 3.

Twelve hours later, the downstream jet streak in Fig. 5 intensified over the warm front, placing the left entrance region over the surface front. This was an unfavorable position to force an updraft ahead of the surface cyclone. A cross section taken through the entrance region of the second jet streak (Fig. 27) illusrates a strong updraft associated with the right entrance region where the broad cloud band south of the jet occurred. It is reasonable to expect a strong, thermally direct circulation to result in a downdraft branch under the left entrance region ahead of the warm front. Instead, a separate updraft was forced by some other mechanism. The deep sloping symmetrically neutral unstable region in Fig. 12 was to the right of this updraft, on the warm front and probably contributed to this ascent. Another possible mechanism for this ascent is PVA associated with the upper trough located over the East Coast.

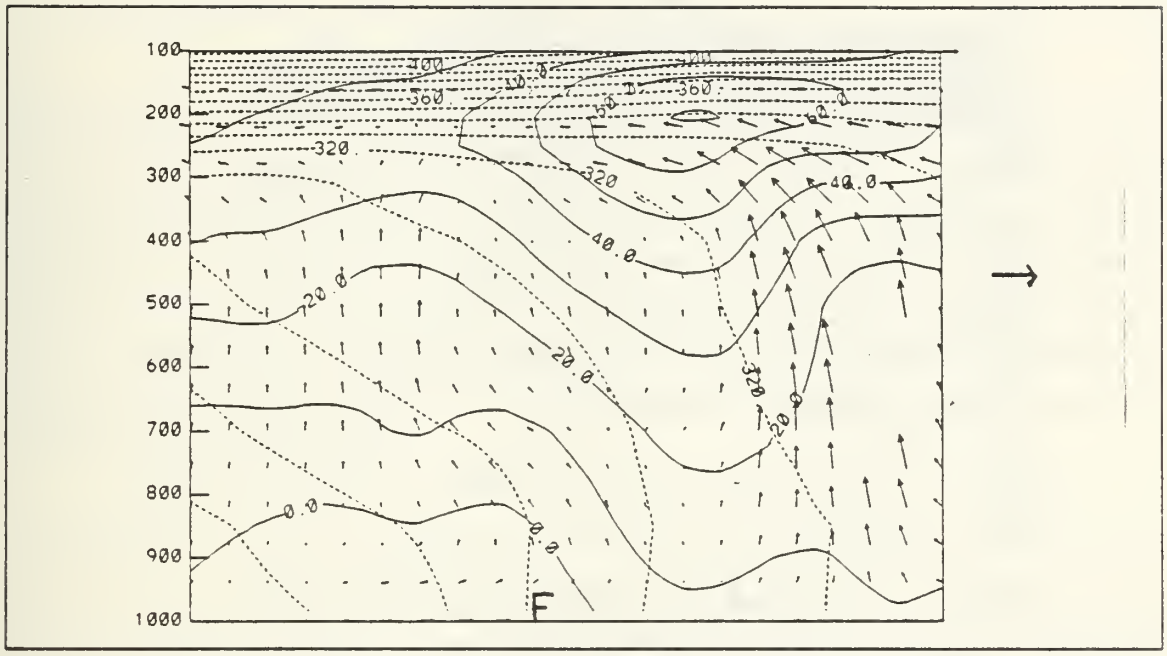

Figure 27. 1200 UTC 25 February 1986 Cross section of isotachs and θ_e: Same as Fig. 26 Location of cross section indicated in Fig. 5.

At 0000 UTC 26 February, the surface cyclone was in its explosive stage. The 250-mb jet streak intensified to the northeast of the surface cyclone over the warm front (Fig. 7), placing the left entrance convergence over the warm front. The right entrance region continued to force a strong updraft (Fig. 28) southeast of the surface cyclone. Again, a downdraft branch would be expected under the left entrance region. Instead, an updraft is present. As discussed above, one possible reason for this updraft is that the low-level forcing was strong enough to overcome the thermally direct circulation associated with the jet and force a strong updraft in this region. The role of the 500-mb PVA in this region forcing the updraft is uncertain.

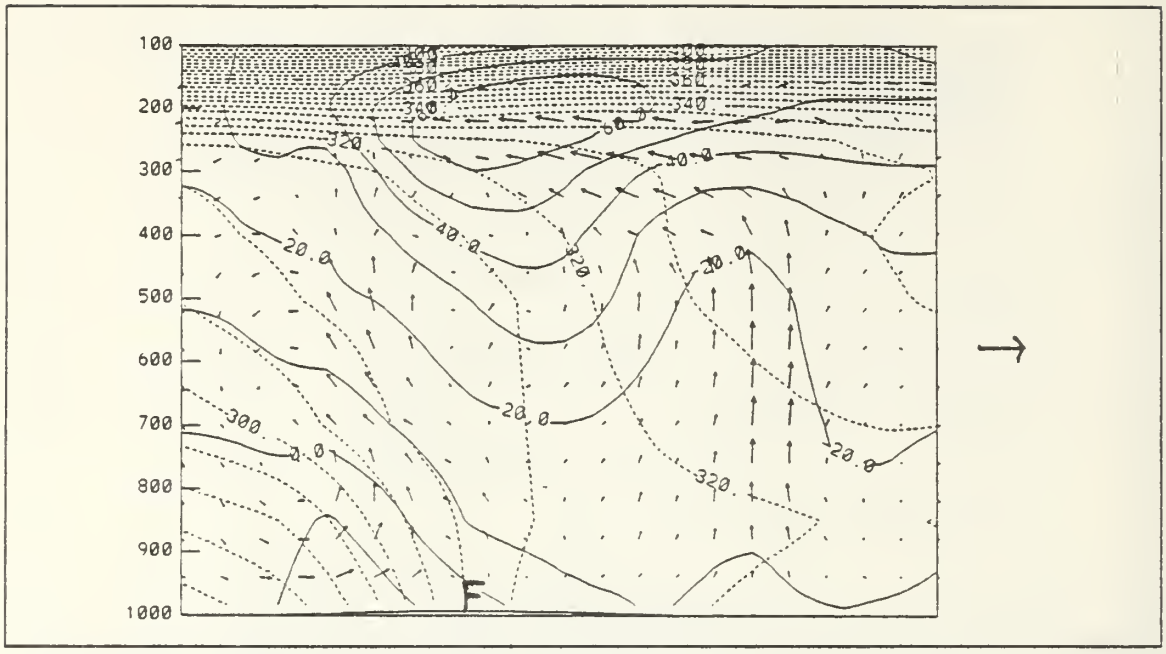

Figure 28. 0000 UTC 26 February 1986 Cross section of isotachs and θ_e: Same as Fig. 26 Location of cross section indicated in Fig. 7.

2. Surface Frontogenesis

Analyses of the jet streak forcing, discussed in the previous section, clearly show that the updraft region ahead of the surface cyclone in IOP9 opposed the upper-level jet stream forcing. An examination of frontogenesis in this case should illustrate the importance of low-level forcing in the updraft. Sanders (1986b and with Bosart, 1985) has studied cases of explosive cyclogenesis which resulted in large amounts of precipitation along the east coast of the United States. In all cases, he determined that the ascent region ahead of the cyclone was driven by large-scale frontogenetic forcing in the presence of small symmetric stability. Emanuel (1988) further suggested that instabilities generated by low-level heating and moistening by surface fluxes and advection of θ_e are neutralized by upper-level increases in θ_e resulting from moist slantwise convection. This slantwise convective adjustment occurs continuously on small time-scales and it reduces the-scale and increases the intensity of the frontogenetically forced updraft.

Frontogenetical forcing was computed by:

$$\frac{d\nabla\theta}{dt} = -|\nabla\theta|^{-1}\{(\frac{\partial u}{\partial x}(\frac{\partial\theta}{\partial x})^2 + \frac{\partial v}{\partial y}(\frac{\partial\theta}{\partial y})^2) + \frac{\partial\theta}{\partial x}\frac{\partial\theta}{\partial y}(\frac{\partial u}{\partial y} + \frac{\partial v}{\partial x})$$

$$+\left(\frac{\partial\theta}{\partial x}\frac{\partial Q}{\partial x}+\frac{\partial\theta}{\partial y}\frac{\partial Q}{\partial y}\right)\}. \qquad (3)$$

The first term on the right, known as horizontal convergence, represents the contribution due to the ageostrophic part of the flow. The second term on the right is the horizontal deformation term, which represents the contribution due to shear and curved geostrophic flow. The last term represents the contribution of differential diabatic heating to creating a temperature gradient. Frontogenetical forcing also includes contributions from a tilting term, which represents the effects of differential vertical motions. Since the tilting term does not contribute to surface frontogenesis, its effect was not considered in this case.

At 0000 UTC 25 February, the updraft region northeast of the cyclone was characterized by a total frontogenetical forcing of 3 K/day/100-km (Fig. 29). Diabatic effects (Fig. 30) slightly opposed frontogenesis. The horizontal convergence term (Fig. 31) contributed more than 2 K/day/100-km, representing almost all of the total forcing in the region. Horizontal deformation accounted for a weak contribution (Fig. 32).

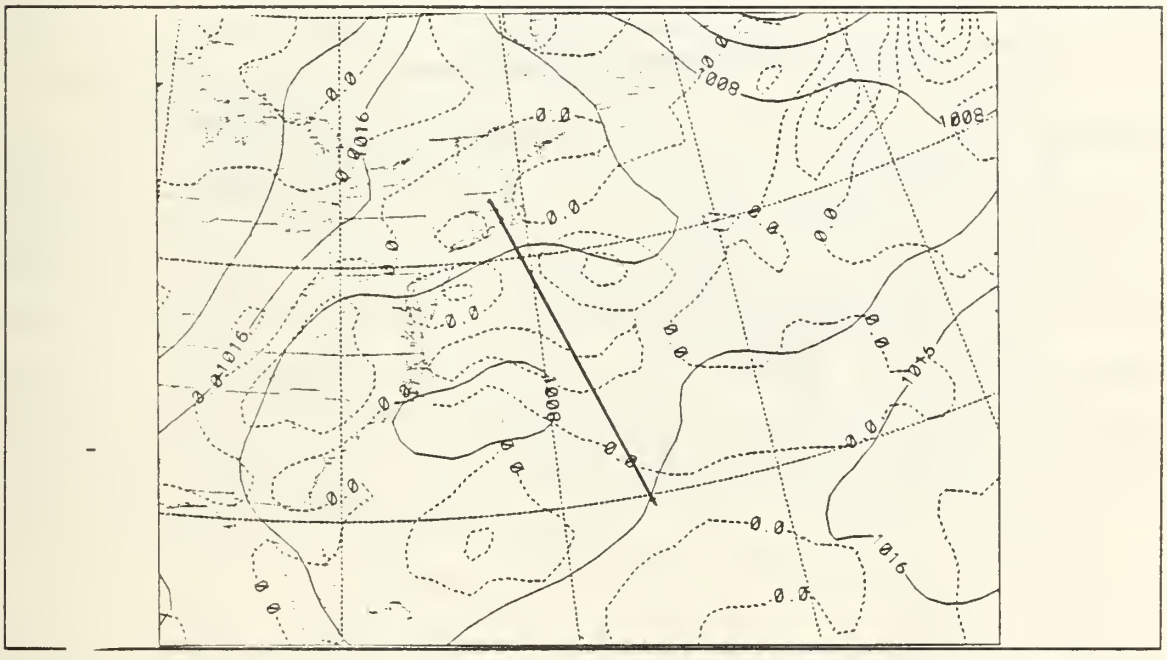

Figure 29. 0000 UTC 25 February 1986 Total frontogenetical forcing: in K day/100-km. Solid lines are sea-level pressure in mb.

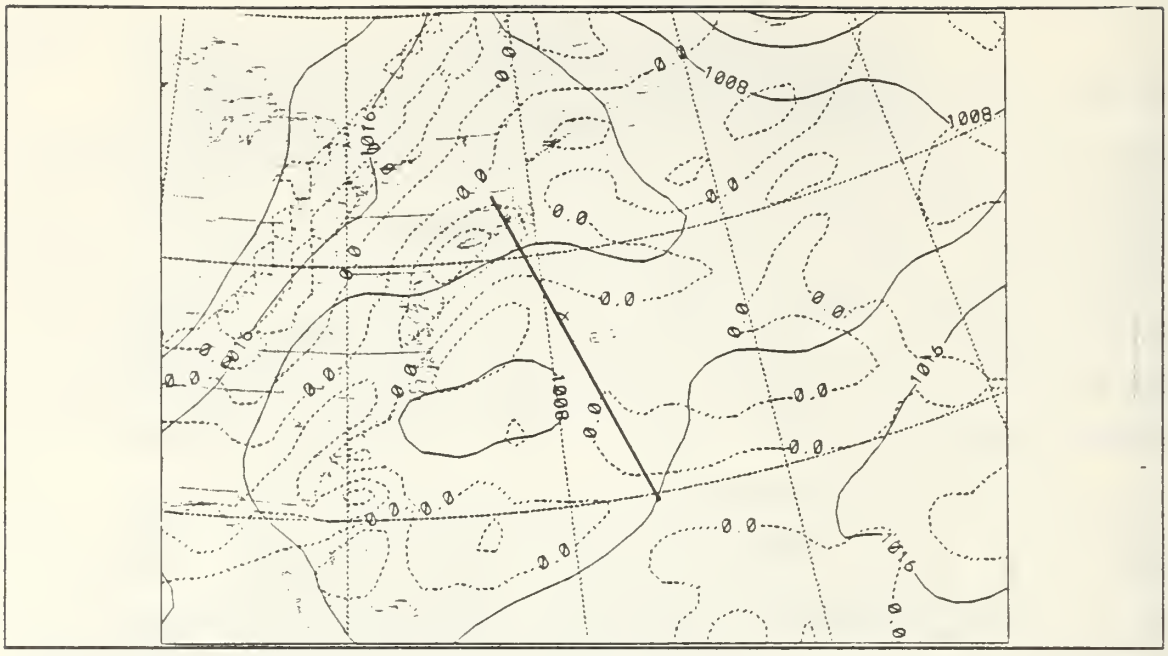

Figure 30. **0000 UTC 25 February 1986 Diabatic term:** K day 100-km. Solid lines are sea-level pressure in-mb.

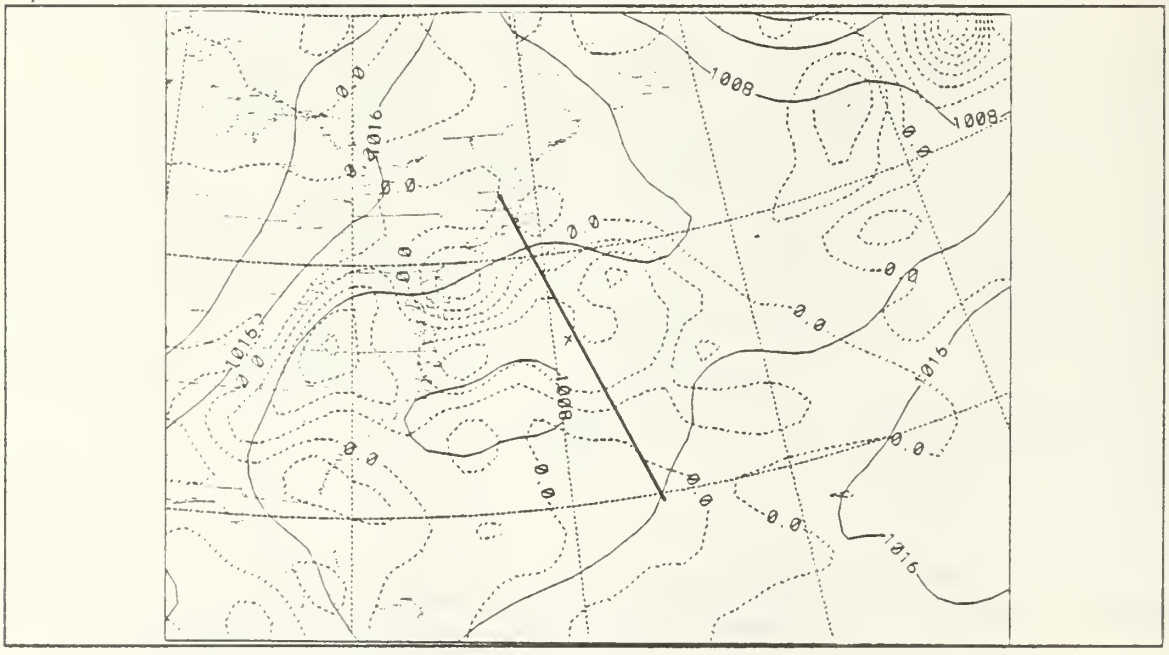

Figure 31. **0000 UTC 25 February 1986 Convergence term:** in K day 100-km. Solid lines are sea-level pressure in-mb.

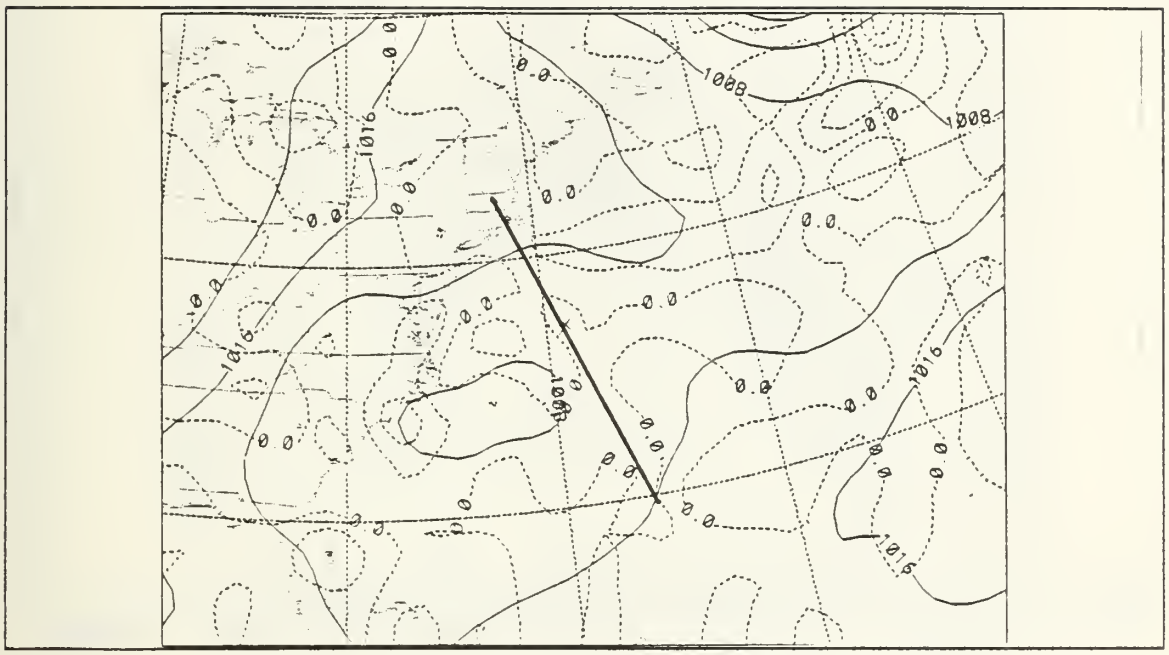

Figure 32. 0000 UTC 25 February 1986 Deformation term: in K day^{-1} 100-km. Solid lines are sea-level pressure in mb.

The 1200 UTC 25 February analyses show an elongated area of frontogenetical forcing to the northeast of the cyclone, associated with the warm front. The maximum total frontogenetical forcing of greater than 6 K day^{-1} 100-km (Fig. 33) was located in the updraft region ahead of the warm front seen in Fig. 27. With decreasing upper-level forcing in this region, it seems evident that the increasing surface forcing along the warm front is contributing significantly to the updraft. The diabatic term (Fig. 34) although no longer opposing frontogenesis, was very small, due to the maximum heat flux being farther south. The convergence and deformation terms (Fig.'s 35 and 36) each contributed nearly half the total forcing.

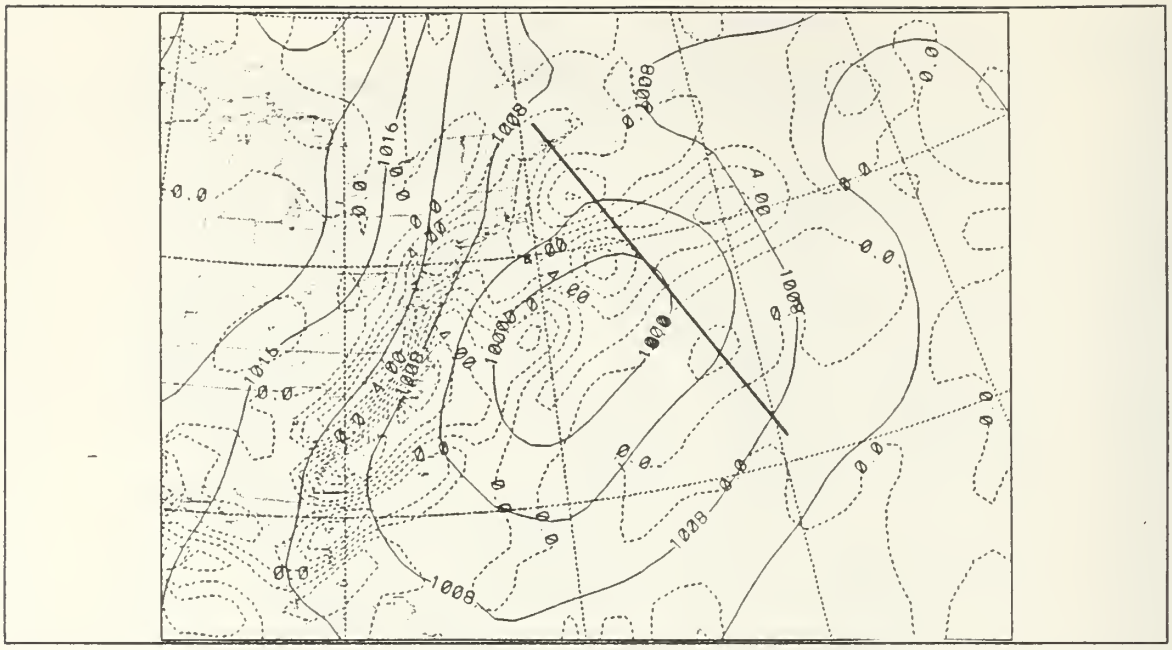

Figure 33. 1200 UTC 25 February 1986 Total frontogenetical forcing: Same as Fig. 29

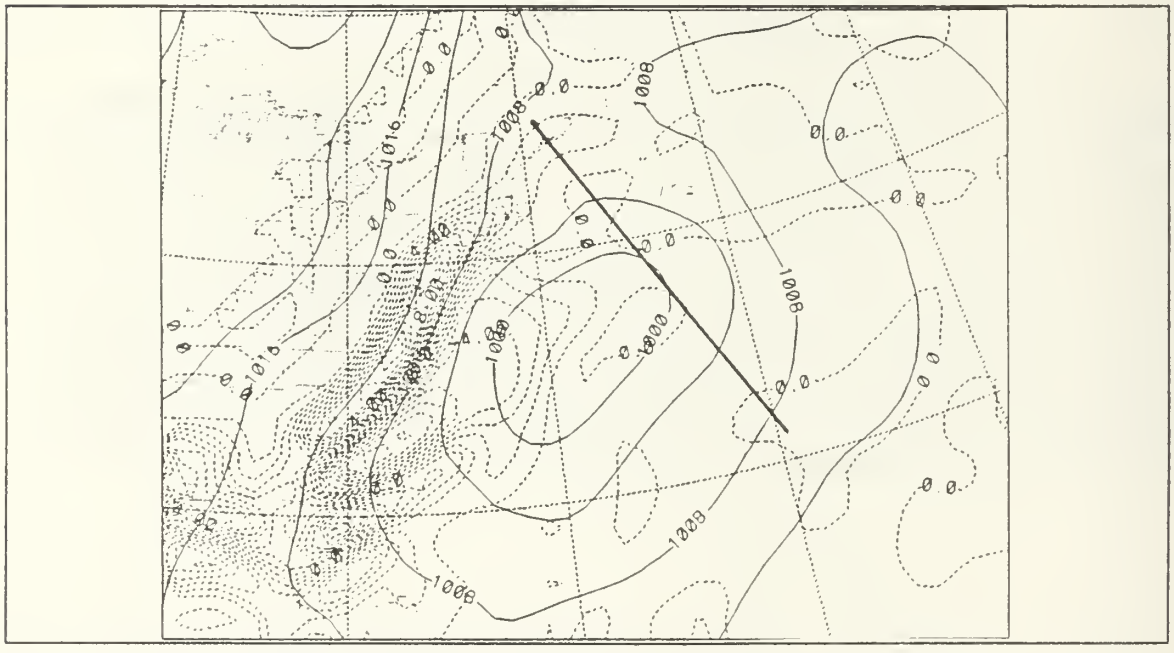

Figure 34. 1200 UTC 25 February 1986 Diabatic term: Same as Fig. 30

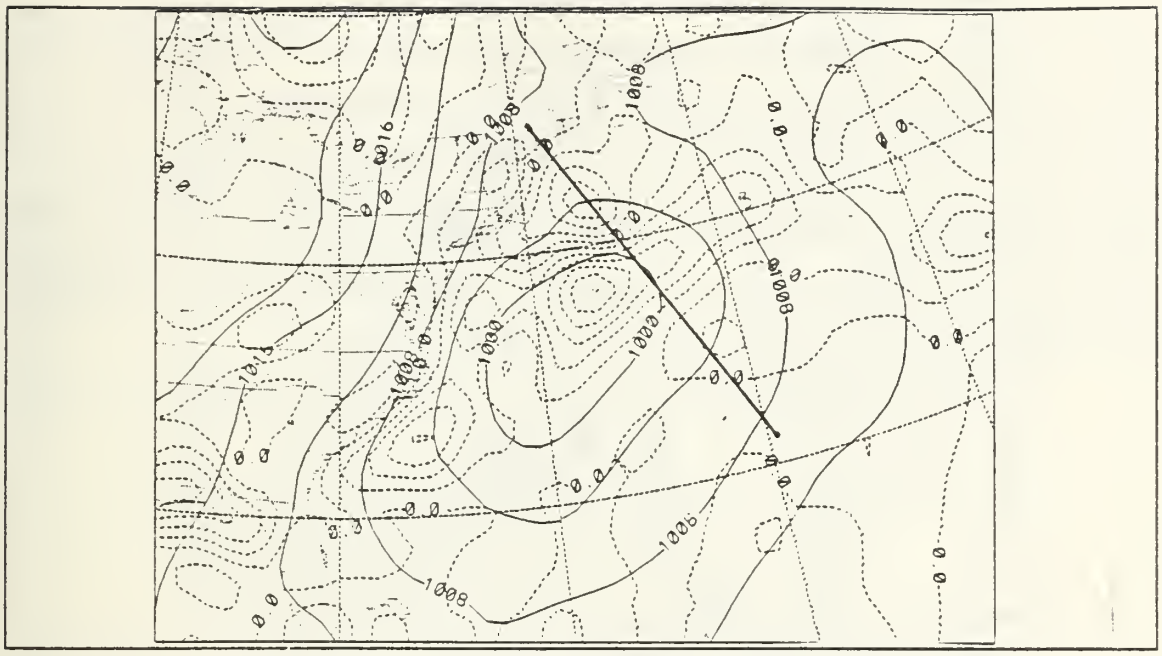

Figure 35. 1200 UTC 25 February 1986 Convergence term: Same as Fig. 31

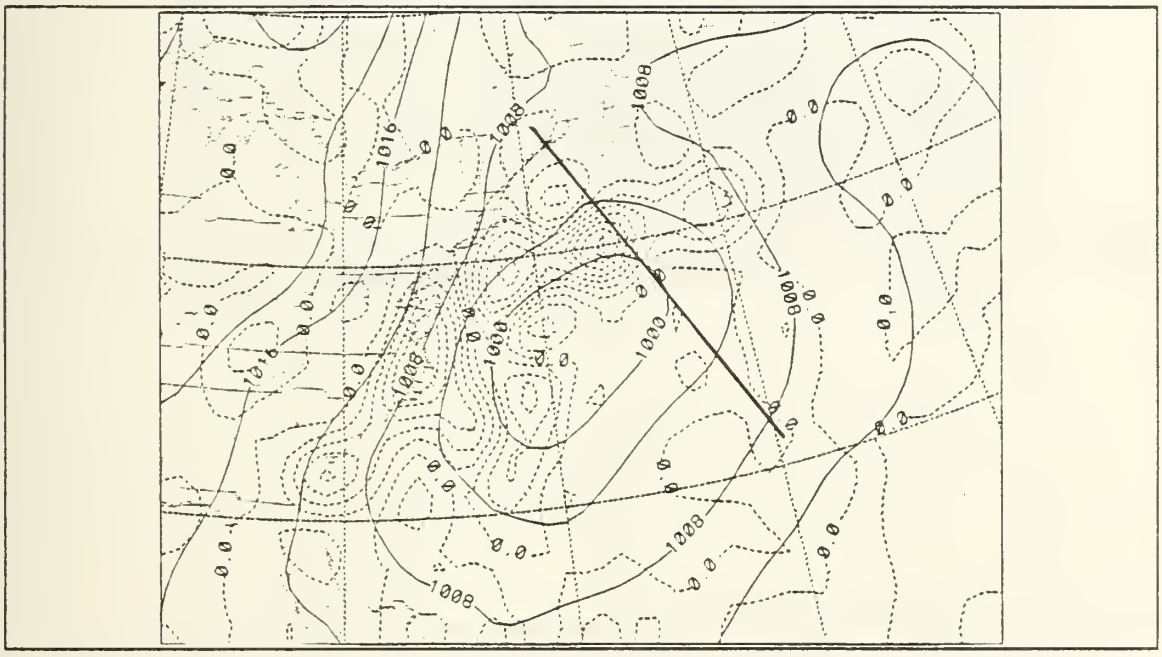

Figure 36. 1200 UTC 25 February 1986 Deformation term: Same as Fig. 32

By 0000 UTC 26 February, the period of maximum deepening of the surface cyclone, the total frontogenetical forcing tripled to a maxumum of 19 K/day/100-km (Fig. 37) in the thermally direct updraft region of the warm front. This confirms the increasing low-level contributions to the warm frontal ascent as suggested in the previous section. The surface heat flux was downward at this time, and consequently the diabatic term opposed frontogenesis by 2 K/day/100-km (Fig. 38). The convergence term (Fig. 39) represented the largest contribution, with a forcing of 12 K/day/100-km. The deformation term (Fig. 40) accounted for 9 K/day/100-km.

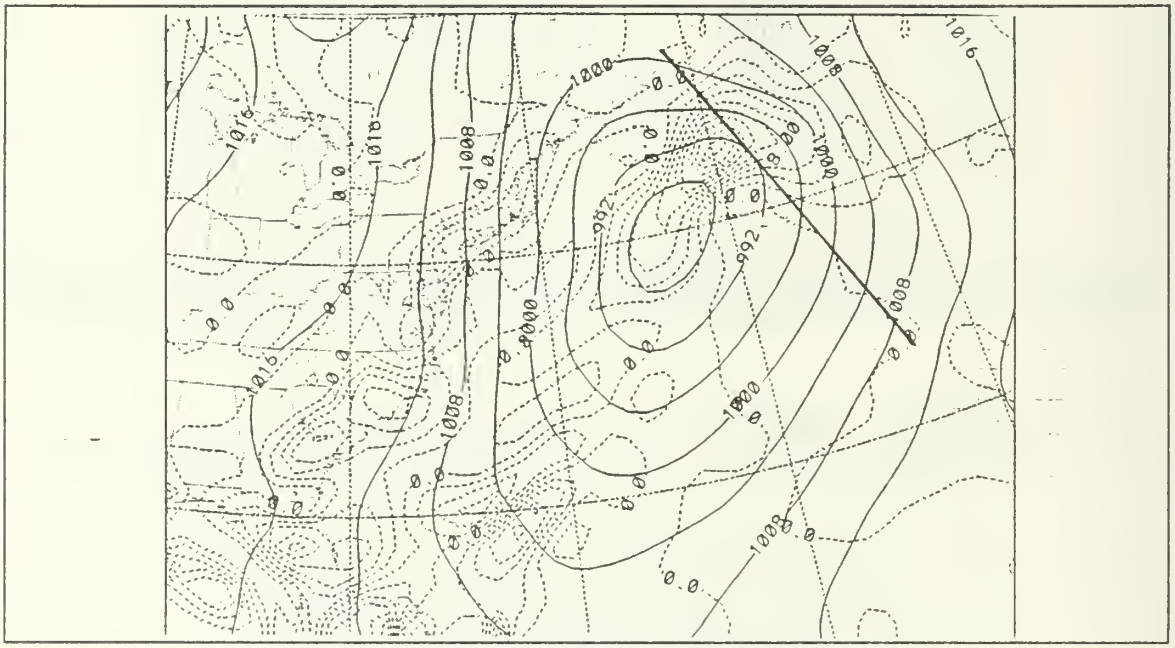

Figure 37. 0000 UTC 26 February 1986 Total frontogenetical forcing: Same as Fig. 29

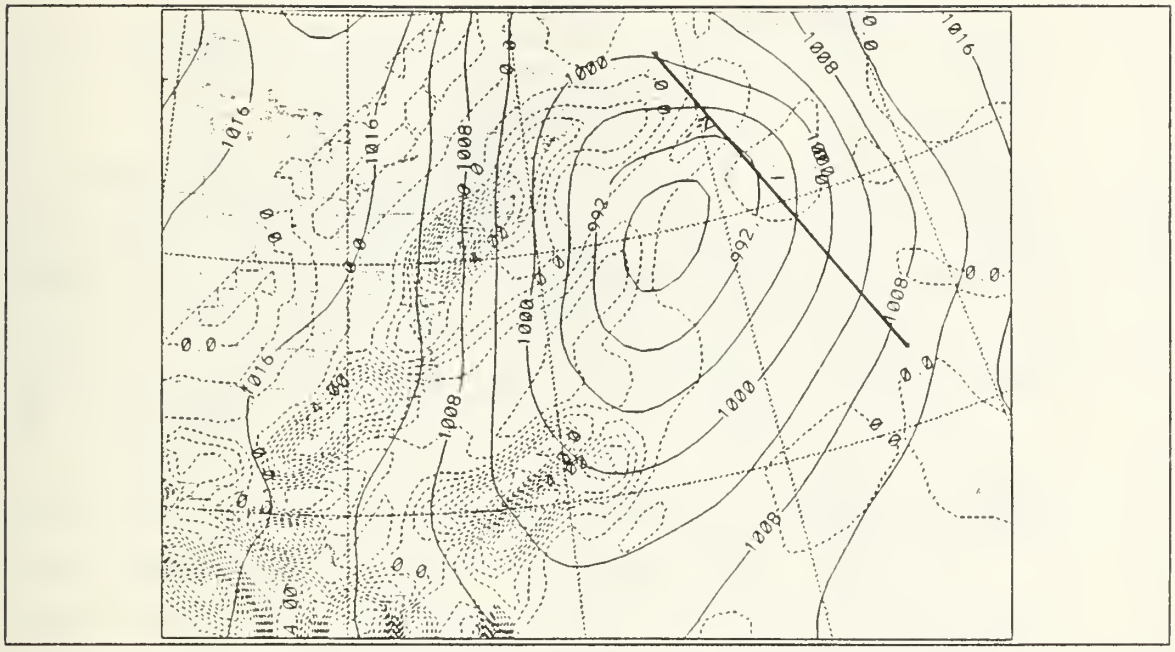

Figure 38. 0000 UTC 26 February 1986 Diabatic term: Same as Fig. 30

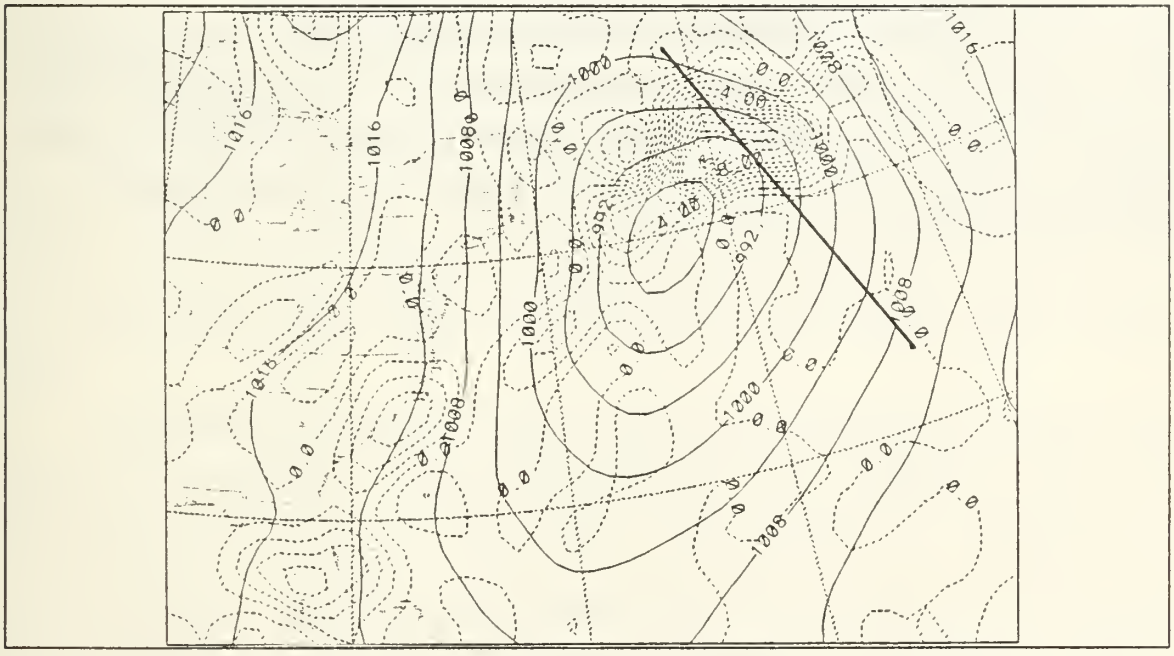

Figure 39. 0000 UTC 26 February 1986 Convergence term: Same as Fig. 31

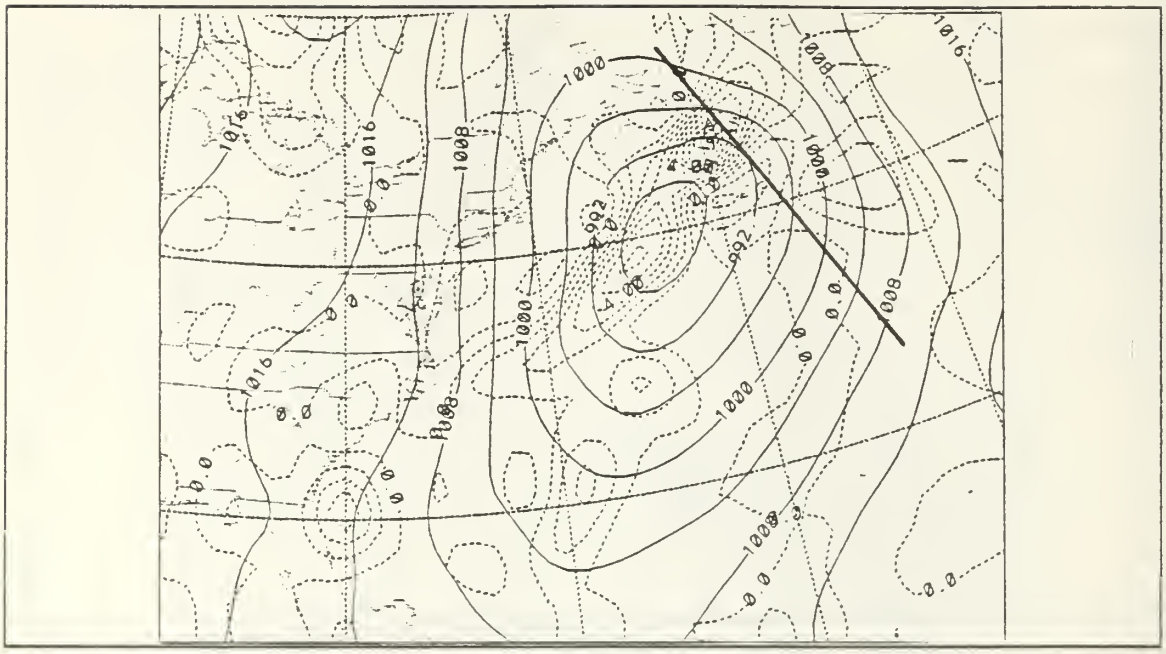

Figure 40. 0000 UTC 26 February 1986 Deformation term: Same as Fig. 32

The frontogenetical forcing in this case was moderate early in the development of the cyclone when jet streak divergence forced the updraft. Later in the period, when the jet streak location became unfavorable to force an updraft, surface frontogenesis increased in strength. During the rapid deepening stage of the surface cyclone, the frontogenetical forcing increased dramatically.

IV. DISCUSSION

Previous studies of explosive cyclogenesis have stressed the importance of upper-level forcing. Sanders (1986a) suggested that large upper-level forcing must be present before low-level forcing can contribute. In their study of an eastern North Pacific cyclone, Reed and Albright (1986) found that rapid deepening occurred in response to the jet stream. Wash et al. (1988) examined two explosive cyclones and found that when the upper-level jet was favorably located, the surface cyclones developed.

The response of the surface cyclone in IOP9 to the upper-level jet stream forcing mechanisms was quite different. Upper-level forcing was a contributing mechanism in forcing the updraft ahead of the surface cyclone early in its development. Low- level forcing provided by frontogenesis enhanced the jet streak induced updraft. The frontogenetical forcing was almost entirely due to horizontal convergence. Later in the period, the 250-mb jet streak was in a position to force a downdraft and inhibit surface development. The frontogenetical forcing, which resulted primarily from horizontal convergence, was strong enough to overcome the thermally direct downdraft. At 0000 UTC 26 February, the frontogenetical forcing increased dramatically and continued to oppose the upper-level forcing, resulting in explosive deepening of the surface cyclone.

Although the details are unclear, it seems apparent that the boundary layer structure played a key role in deforming the thermal field and increasing surface frontogenesis ahead of the cyclone in this case. This suggests that PBL processes were important in providing a favorable prestorm environment which set the stage for explosive development.

In the Presidents' Day storm, Bosart and Lin (1984) concluded that surface fluxes and cold air damming were vital to setting up strong coastal frontogenesis. In that case, differences between the land and water surfaces were responsible for the frontogenesis. Cold air advection resulted in differential heat fluxes along the coast. Differences in roughness between the land and water increased the frictional convergence along the front. Surface frontogenesis in IOP9 was forced primarily by convergence in the PBL.

Development occurred well offshore, where there were no differences in surface roughness to cause frictional convergence. Nuss (1989) suggests that PBL convergence is enhanced by differences in horizontal boundary layer stratification in the warm frontal regions of cyclones over the open ocean, which potentially explains the strong

ageostrophic frontogenesis in this case. In addition , the symmetrically neutral frontal region may have enhanced the updraft and ageostrophic frontal circulation as suggested by Emanuel (1985), which in turn increased the frontogenesis.

Surface fluxes directly contributed to development only in the early stages of cyclogenesis, when the fluxes resulted in heating and moistening the boundary layer. This is consistent with the results of Green (1988), who showed that the warm moist air was confined to near the surface by a lid of warm dry air. He found that this lid inhibited free convection which prevented latent heat from being released. As the updraft increased in intensity and the lid eroded, high θ_e air was advected upward and latent was released.

To maintain symmetric neutrality, surface θ_e increases must result in θ_e increases aloft. Moist slantwise convection in the ascending air provided sufficient latent heat release to increase θ_e above the surface. The moist slantwise convective adjustment continuously neutralized the atmosphere and enhanced the updraft.

Because the model used in this study cannot resolve details of small-scale features and because the moisture fields are 12-h forecasts, the computations used in this study contain some uncertainties. The largest uncertainties exist in the PBL θ_e computations, as well as the cross-sectional θ_e analyses. Even with potentially large errors, the θ_e analyses were consistent with actual data where they were available. Therefore, conclusions drawn from the θ_e analyses are considered credible.

V. CONCLUSIONS AND RECOMMENDATIONS

A. CONCLUSIONS

The development of the surface cyclone in IOP9 was not consistent with other cases of oceanic cyclogenesis. Upper-level forcing contributed to development in the early stages but inhibited development later. Instead of decaying, the surface cyclone continued to develop and in fact deepened explosively in response to frontgenetical forcing in a symmetrically neutral environment.

The atmosphere in the warm frontal region ahead of the surface cyclone in GALE IOP9 was characterized by small, nearly neutral symmetric stability. On a cross section taken through a cloudy region near the surface cyclone center, surfaces of pseudo-absolute momentum, M and equivalent potential temperature, θ_e, were nearly parallel. A sounding located along the cross section was evaluated for symmetric stability using the procedure developed by Emanuel (1983). The sounding supported the cross section by indicating near symmetric neutrality in the cloudy region. Since both methods of evaluation concur, the cross section method is valid in this case, at least near the sounding. Cross sections of M and θ_e taken through the updraft region ahead of the cyclone indicate that the atmosphere in the updraft region was symmetrically neutral throughout the period.

In a symmetrically neutral atmosphere, local changes in θ_e determine the development of a moist baroclinic cyclone. Examining the terms that contribute to heating and moistening the planetary boundary layer, it was apparent that surface heat and moisture flux divergence accounted for nearly half of the increases in θ_e early in the development of the cyclone. As the cyclone moved over colder water, the surface fluxes became negative and horizontal advection of θ_e represented the total contribution to heating and moistening the boundary layer.

Isolating the upper-level jet stream and low-level mechanisms that forced the updraft ahead of the surface cyclone, it is apparent that the jet streak drove the ascent only in the early period of development. Later, the intensifying jet streak was in a position to force a downdraft in the region. Surface frontogenesis may have been strong enough to oppose the thermally direct circulation and force a strong updraft ahead of the surface cyclone. The role of the upstream 500 mb trough in forcing this updraft is uncertain.

B. RECOMMENDATIONS

Since the conlusions drawn from this study represent a single case, it is recommended that other cases of oceanic cyclogenesis be examined to determine the importance of low-level forcing. Data sets from the current Experiment on Rapid Cyclogenesis in the Atlantic (ERICA) should provide excellent opportunities for further study using more detailed data sets. Several limitations were noted in the analyses used for this case. Since moisture analyses are vital to this study, accurate moisture data should be used instead of a first guess.

Cross sections constructed from actual soundings would describe the atmosphere better than those constructed from gridded model data. Cross sections should be made from four or five soundings to provide sufficient detail over a large area.

It was apparent in this case that understanding the boundary layer structure is critical to understanding the surface development. Reconstruction of the frontal response in IOP9 through various solutions to the Sawyer-Eliassen equation may be helpful to understand the role of boundary layer stratification in enhancing the ageostrophic frontogenesis as well as the effect of symmetric neutrality on the frontal circulation. In addition to detailed diagnostic studies of IOP9, various model forecast runs may isolate the roles of PBL processes. Varying the intensities of heat and moisture fluxes in the initialization stage may help explain their contributions. The inclusion of detailed sea-surface temperature analyses may offer more information on the PBL structure.

LIST OF REFERENCES

Atlas, R., 1987: The role of oceanic fluxes and initial data in the numeral prediction of an intense coastal storm. *Dynamics of Atmospheres and Oceans,*10, 359-388.

Bennetts, D.A., and B.J Hoskins, 1979: Conditional symmetric instability - a possible explanation for frontal rainbands. *Quart. J. Roy. Meteor. Soc.,*105, 945-962.

Bosart, L.F., and S.C. Lin, 1984: A diagnostic analysis of the Presidents' Day storm of February 1979. *Mon. Wea. Rev.,* 112, 2148-2177.

Boyle, J.S., and L.F. Bosart, 1986: Cyclone-anticyclone couplets over North America Part II: Analysis of a major cyclone event over the Eastern United States. *Mon. Wea. Rev.,*114, 2432-2465.

Brown, R.A., and W.T. Liu, 1982: An operational large-scale marine planetary boundary layer model. *J. Appl. Meteor.,*21, 261-269.

Carson, J.L., 1988: A study of a rapid cyclogenesis event during GALE, M.S. thesis, Naval Postgraduate School, Monterey, California, 74 pp.

Davis, C.A., and K.A. Emanuel, 1988: Observational evidence for the influence of surface heat fluxes on rapid maritime cyclogenesis. *Mon. Wea. Rev.,* 116,2649-2651.

Emanuel, K.A., 1983: On assessing local conditional symmetric instability from atmospheric soundings. *Mon. Wea. Rev.,* 111,2016-2033.

------, 1985: Frontal circulations in the presence of small moist symmetric stability. *J. Atmos. Sci.,* 42, 1062-1071.

------, 1988: Observational evidence of slantwise convective adjustment *Mon. Wea. Rev.,* 116,1805-1816.

Genesis of Atlantic Lows Experiment (GALE) Field Program Summary, 1986: GALE Data Center, Drexel University, Department of Physics and Atmospheric Science, Philadelphia, Pennsylvania, 152 pp.

Green, C.W., 1988: Possible contributions of lid conditions during explosive cyclogenesis, M.S. thesis, Naval Postgraduate School, Monterey, California, 99 pp.

Holton, J.R., 1979:*An Introduction to Dynamic Meteorology,* Academic Press, New York, 391 pp.

Hoskins, B.J., M.E. McIntyre and A.M. Robertson, 1985: On the use and significance of isentripic potential vorticity maps. *Quart. J. Roy. Meieor. Soc.,* 111, 877-946.

Nuss, W.A., 1989: Air-sea interaction influences on the structure and intensification of an idealized marine cyclone. *Mon. Wea. Rev.,* 117, 351-369.

------, and S.I. Kamikawa, 1988: Dynamics and low-level processes in two Asian cyclones. Manuscript to be submitted to *Mon Wea. Rev.*.

Pertle, W.E., 1987: A synoptic investigation of maritime cyclogenesis during GALE. M.S. thesis, Naval Postgraduate School, Monterey, California, 103 pp.

Reed, R.J., and M.D. Albright, 1986: A case study of explosive cyclogenesis in the eastern Pacific. *Mon. Wea. Rev.*, 114, 2297-2319.

Sanders, F., 1986a: Explosive cyclogenesis in the West Central North Atlantic Ocean, 1981-1984. Part I: Composite structure and mean behavior. *Mon. Wea. Rev.*,114,1781-1794.

-------, 1986b: Frontogenesis and symmetric stability in a major New England snowstorm. *Mon. Wea. Rev.*,114,1847-1862.

Sanders, F., and L. Bosart, 1985: Mesoscale structure in the megalopolitan snowstorm of 11-12 February 1983. *J. Atmos. Sci.*, 42, 1050-1061.

-------, and J.R. Gyakum, 1980: Synoptic-dynamic climatology of the "bomb". *Mon. Wea. Rev.*,108,1589-1606.

Uccellini, L.F., D. Keyser, K.F. Brill and C.H. Wash, 1985: The Presidents' Day cyclone of 18-19 February 1979: Influence of upstream trough amplification and associated tropopause folding on rapid cyclogenesis. *Mon. Wea. Rev.*,113,962-988.

------, R.A. Petersen, K.F. Brill, P.J. Kocin and J.J. Tuccillo, 1987: Synergistic interactions between an upper level jet streak and diabatic processes that influence the development of a low level jet and a secondary coastal cyclone. *Mon. Wea. Rev.*, 115, 2227-2261.

Wash, C.H., J.E. Peak, W.E. Calland and W.A. Cook, 1988: Diagnostic study of explosive cyclogenesis during FGGE. *Mon. Wea. Rev.*, 116, 431-451.

------, S.L. Heikkinen, C.-S. Liou, W.A. Nuss and R.L. Elsberry, 1989: Study of the rapid cyclogenesis during GALE IOP9. Manuscript to be submitted to *Mon. Wea. Rev.*.

Whittaker, J.S., L.W. Uccellini and K.F. Brill, 1988: A model-based diagnostic study of the rapid development phase of the Presidents' Day cyclone. *Mon. Wea. Rev.*,116,2337-2365.

INITIAL DISTRIBUTION LIST

		No. Copies
1.	Defense Technical Information Center Cameron Station Alexandria, VA 22304-6145	2
2.	Library, Code 0142 Naval Postgraduate School Monterey, CA 93943-5002	2
3.	Chairman (Code 63Rd) Department of Meteorology Naval Postgraduate School Monterey, CA 93943-5000	1
4.	Chairman (Code 68Co) Department of Oceanography Naval Postgraduate School Monterey, CA 93943-5000	1
5.	Professor Carlyle H. Wash (Code 63WX) Department of Meteorology Naval Postgraduate School Monterey, CA 93943-5000	2
6.	Professor Wendell A. Nuss (Code 63NU) Department of Meteorology Naval Postgraduate School Monterey, CA 93943-5000	5
7.	Professor Russell E. Elsberry (Code 63ES) Department of Meteorology Naval Postgraduate School Monterey, CA 93943-5000	1
8.	Lt. Dianne K. Crittenden, USN NOCC/JTWC COMNAVMARIANAS Box 12 FPO San Francisco, CA 96630	1
9.	Director Naval Oceanography Division Naval Observatory 34th and Massachusetts Avenue NW Washington, DC 20390	1
10.	Commander Naval Oceanography Command Stennis Space Center, MS 39529-5000	1

11. Commanding Officer
Naval Oceanographic Office
Stennis Space Center, MS 39522-5001 — 1

12. Commanding Officer
Fleet Numerical Oceanography Center
Monterey, CA 93943 — 1

13. Commanding Officer
Naval Environmental Prediction Research Facility
Monterey, CA 93943 — 1

14. Chairman, Department of Atmospheric Science
University of Missouri
Columbia, MO 65201 — 1

15. Chief of Naval Research
800 North Quincy Street
Arlington, VA 22217 — 1

16. Office of Naval Research (Code 420)
Naval Ocean Research and Development Activity
800 North Quincy Street
Arlington, VA 22217 — 1

Thesis
C8734 Crittenden
c.1 Thermodynamic and
dynamic processes in
the updraft region of
GALE IOP9.